NASA TN D-1772

TECHNICAL NOTE

D-1772

STUDY OF INERTIAL NAVIGATION ERRORS DURING REENTRY

TO THE EARTH'S ATMOSPHERE

By Q. Marion Hansen, John S. White,
and Albert Y. K. Pang

Ames Research Center
Moffett Field, Calif.

NATIONAL AERONAUTICS AND SPACE ADMINISTRATION

WASHINGTON

May 1963

TABLE OF CONTENTS

SUMMARY 1

INTRODUCTION 1

NOTATION 2

PROCEDURE 4

General Method 4

Equations for Actual and Indicated Motion 6

Partial Derivative Equations for Linear Error Analysis 9

Trajectory Parameters and Vehicle Characteristics 11

Initial Condition and Equipment Errors 13

RESULTS AND DISCUSSION 13

Range of Linearity 14

Use of Partial Derivatives for Estimating Final Errors 16

CONCLUDING REMARKS 19

APPENDIX - DERIVATION OF PARTIAL DERIVATIVES FOR AN ELLIPSE 20

REFERENCES 23

TABLES 24

FIGURES 33

NATIONAL AERONAUTICS AND SPACE ADMINISTRATION

TECHNICAL NOTE D-1772

STUDY OF INERTIAL NAVIGATION ERRORS DURING REENTRY TO THE EARTH'S ATMOSPHERE

By Q. Marion Hansen, John S. White,
and Albert Y. K. Pang

SUMMARY

The navigation errors in position and velocity which result from erroneous initial conditions and imperfect inertial navigation equipment have been analyzed for a space vehicle reentering the earth's atmosphere. The analysis has shown that for realistic errors and reentry conditions a linear error analysis will usually be valid; that is, the partial derivatives of final position and velocity with respect to initial conditions and equipment parameters may be treated as constants. Also, the analysis has demonstrated that these partial derivatives can be used to estimate the final errors which result from using various combinations of initial condition and equipment errors with the inertial navigation process started at various times before reentry.

It was found that when the inertial navigation process is started just prior to reentry the final errors resulting from initial condition errors predominate, but when started well before reentry the final errors resulting from equipment errors predominate. Initial altitude error is the most significant initial condition error, and accelerometer bias and gyro drift are the most significant equipment errors. The final errors due to accelerometer bias may be greatly reduced by treating the outputs of the accelerometers as zero above the atmosphere.

INTRODUCTION

If a vehicle reentering the earth's atmosphere is to reach a particular landing site, it is desirable to have continuous knowledge of position, velocity, and attitude of the vehicle. To provide this information for a reentry vehicle, especially one with a pilot, an inertial navigation system is generally considered essential, since continuous radio reception of ground data is very difficult (if not impossible) and since it is very desirable, from a reliability standpoint, to have an accurate, self-contained navigation system on board the vehicle.

In any inertial navigation system, navigation errors in instantaneous position and velocity result from both erroneous initial conditions and imperfect

inertial navigation equipment. These navigation errors during reentry from a circular orbit into the atmosphere of a spherical, rotating earth were studied in reference 1. The present study extends the analysis of reference 1 to include partial derivatives. The use of partial derivatives for predicting navigation errors which result from only initial condition errors for nonatmospheric reentry is fairly common (ref. 2, p. 736, for example). The present report uses partial derivatives to examine the navigation errors in position and velocity which result when an inertial navigation system is used during reentry into the atmosphere of a spherical rotating earth.

There are two main objectives of this report. The first is to determine the range of values of initial condition and equipment errors over which a linear error analysis is valid, that is, to determine the range over which partial derivatives of final position and velocity with respect to initial conditions and equipment parameters remain constant. The second objective is to demonstrate within the linear range the use of these partial derivatives for estimating the final errors which result from using various combinations of initial condition and equipment errors with the inertial navigation system "started" at various times before reentry.[1]

In this study, a lunar trajectory is used as an example; however, it will be shown that a linear analysis should be valid for any realistic errors and reentry conditions. Furthermore, the same error relationships should exist between the relative effects of initial condition and equipment errors upon the final errors for any realistic errors and reentry conditions.

NOTATION

A	reference area for aerodynamic force coefficients, km^2
a	semimajor axis of an ellipse, km
C_D	drag coefficient
$\frac{C_D A}{m}$	vehicle constant relating drag per unit mass to airspeed and air density, 4.1×10^{-9} km^2/kg
D	aerodynamic drag per unit mass, km/sec^2
E	eccentric anomaly of an ellipse, radians
e	eccentricity of an ellipse
f	acceleration, or nongravitational force per unit mass, km/sec^2

[1]In this report the inertial navigation system is considered to be "started" when the last set of initial conditions is put into the system, that is, when the system is updated for the last time prior to reentry.

g	$\frac{\mu}{r_E^2}$, gravitational attraction of earth per unit mass at earth's surface, 9.798597×10^{-3} km/sec^2
H	angular momentum per unit mass, km^2/sec
h	altitude above mean sea level, km
L	aerodynamic lift per unit mass, km/sec^2
m	total mass of vehicle, kg
r	radial distance to vehicle from center of earth, km
r_E	radius of the earth, 6378.14 km
r_p	radius of perigee of an elliptical orbit, km
S	accelerometer scale factor uncertainty, g/g
SF	accelerometer scale factor, g/g
t	time, measured positive after start time, min
t_p	time for a vehicle to travel from r to r_p on an ellipse, min
t'	time after reentry, measured positive after reentry at h = 121.92 km or 400,000 ft, min
U	accelerometer bias, g
V	velocity of vehicle in inertial space, km/sec
V_A	velocity of vehicle relative to the air mass, km/sec
γ	inertial flight-path angle, angle from true horizontal to $\bar{V}$, positive up, radians
γ_A	flight-path angle, angle from true horizontal to $\bar{V}_A$, positive up, radians
θ	range angle, angle between $\bar{r}$ for h = 121.92 km and instantaneous $\bar{r}$, positive from west to east, radians
θ_a	accelerometer misalinement angle, angle between inertial reference axes and accelerometer axes, radians
$\dot{\theta}_E$	angular rate of earth's rotation, 7.292115×10^{-5} radian/sec
μ	gravitational constant for earth, 3.986135×10^5 km^3/sec^2
ρ	atmosphere density, kg/km^3

Subscripts

e	instantaneous error, found by subtracting actual value from indicated value
f	final value, at time final altitude of 30 km is reached
i	indicated value, given by inertial navigation system
o	start value, when initial conditions are put into system
R	value at reentry, where h = 121.92 km
x,z, etc.	value along the x, z, etc., axis
$(\bar{\ })$	vector
$(\dot{\ })$	time derivative

Matrices

[F]	final error matrix
[P]	partial derivative matrix
[S]	initial, or start, error matrix

Two-Dimensional Coordinates

r,θ	earth-centered, polar
x,z	vehicle-centered, actual horizontal and vertical
x_a,z_a	accelerometer axes, which differ from inertial axes because of misalinement
x_i,z_i	vehicle-centered, indicated horizontal and vertical
x_I,z_I	inertial reference axes, which are horizontal and vertical at start time

PROCEDURE

General Method

The general method used to study the navigation errors that result from the inaccuracies of an inertial navigation system used during reentry was to solve concurrently equations for the actual motion and for the indicated motion of the vehicle. Typical actual and indicated trajectories are shown in polar

coordinates in sketch (a), where the separation between the actual and indicated trajectories has been exaggerated for illustrative purposes. The indicated motion, given by the inertial navigation system, differs from the actual motion because of inaccurate knowledge of initial position and velocity and also because of imperfect inertial navigation equipment. The equations were solved with an IBM 7090 computer, and the instantaneous errors were computed after each integration step by subtracting the actual values of position and velocity from the indicated values. The final errors were taken as the errors in position and velocity at a time corresponding to an actual final altitude of 30 km. This final altitude was chosen because ground-based radio contact may easily be made at this altitude, and also because it is anticipated that a parachute or other landing device will be used at or near this altitude.

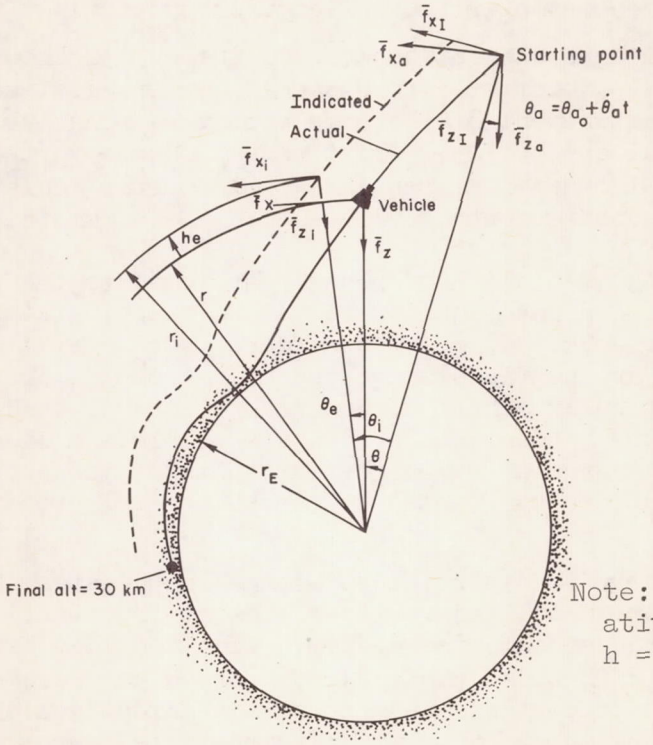

Note: θ and θ_i are negative until reentry at h = 121.92 km.

Force components represented in inertial, accelerometer, indicated, and actual coordinate systems.

Sketch (a)

The instantaneous errors in altitude and range angle, h_e and θ_e, respectively, are illustrated in sketch (a). Of primary interest in this report are the final errors listed below.

Final Errors

h_{ef}	Altitude error
θ_{ef}	Range angle error
$\dot{h}_{ef}$	Altitude rate error
$\dot{\theta}_{ef}$	Range angle rate error

The final errors were assumed to result from the following initial condition and equipment errors.

Initial Condition Errors

h_{e_o}	Altitude error
θ_{e_o}	Range angle error
$\dot{h}_{e_o}$	Altitude rate error
$\dot{\theta}_{e_o}$	Range angle rate error

Equipment Errors

θ_{a_o}	Accelerometer misalinement angle
$\dot{\theta}_a$	Gyro drift rate
U_{x_a}, U_{z_a}	Accelerometer biases
$\Delta S_{x_a}, \Delta S_{z_a}$	Accelerometer scale factor uncertainties

The initial condition errors exist because of inaccurate knowledge of position and velocity. For the equipment errors accelerometer misalinement angle represents the initial misalinement of the accelerometers relative to their reference directions in inertial space. Gyro drift rate produces further accelerometer misalinement and accelerometer biases and accelerometer scale factor uncertainties cause the accelerometer output values to differ from their input values.

For simplicity the vehicle motion was restricted to the east direction in the equatorial plane of a spherical earth with a rotating atmosphere. Crossrange motion and crossrange errors were not considered for several reasons: first, reentry trajectories are nearly planar; second, errors in crossrange are largely functions of the particular scheme of crossrange control used; and third, for a nearly planar trajectory, crossrange errors are stable and also independent of altitude and downrange errors. Hence, the results of the analysis for errors in altitude and downrange are unaffected by the absence of crossrange motion.

Also for simplicity the inertial reference coordinates shown in sketch (a) were chosen as the horizontal and vertical axes at the starting point where the initial conditions are put into the system. Also the accelerometer axes were assumed to be alined with these axes, except for an accelerometer misalinement angle, θ_a. Hence, no attempt was made to obtain an optimum alinement of the gyros or accelerometers in order to minimize the final errors. The accelerometer misalinement angle, θ_a, was assumed to be composed of an initial term, θ_{a_o}, and a time-increasing term, $\dot{\theta}_a t$. The time-increasing term was assumed to be entirely due to gyro drift, so that $\dot{\theta}_a$ is referred to as gyro drift rate.

Equations for Actual and Indicated Motion

The actual motion of the vehicle is described by the equations of motion for one body moving around another. In polar coordinates, r and θ, illustrated in sketch (b), these equations are (ref. 3, p. 42):

$$\left.\begin{aligned} \ddot{r} - r\dot{\theta}^2 &= -\frac{\mu}{r^2} - f_Z \\ r\ddot{\theta} + 2\dot{r}\dot{\theta} &= f_X \end{aligned}\right\} \qquad (1)$$

where μ/r^2 is the gravitational attraction per unit mass at radius, r, and f_x and f_z are the components of lift and drag (and thrust if used) per unit mass in the horizontal and vertical directions, respectively. Sketch (c) may be used to resolve lift and drag into

$$\left.\begin{aligned} f_x &= -D\left(\cos\gamma_A + \frac{L}{D}\sin\gamma_A\right) \\ f_z &= D\left(\sin\gamma_A - \frac{L}{D}\cos\gamma_A\right) \end{aligned}\right\} \tag{2}$$

where

$$D = \frac{1}{2}\rho V_A^2 \frac{C_D A}{m} \tag{3}$$

Equations for γ_A and V_A may be written directly from sketch (c).

$$\left.\begin{aligned} \gamma_A &= \tan^{-1}\frac{\dot{r}}{r(\dot{\theta} - \dot{\theta}_E)} \\ V_A &= \sqrt{\dot{r}^2 + r^2(\dot{\theta} - \dot{\theta}_E)^2} \end{aligned}\right\} \tag{4}$$

Equations (1) through (4) were used to solve for the actual motion of the vehicle.

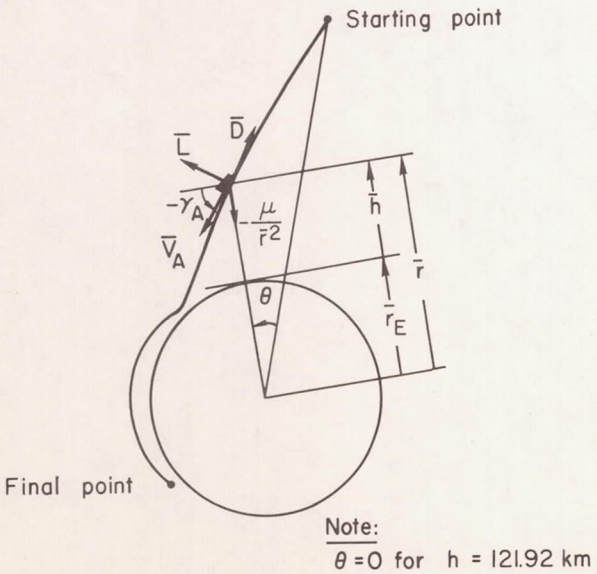

Reentry trajectory in polar coordinates showing lift, drag, gravity, velocity, and flight-path angle.

Sketch (b)

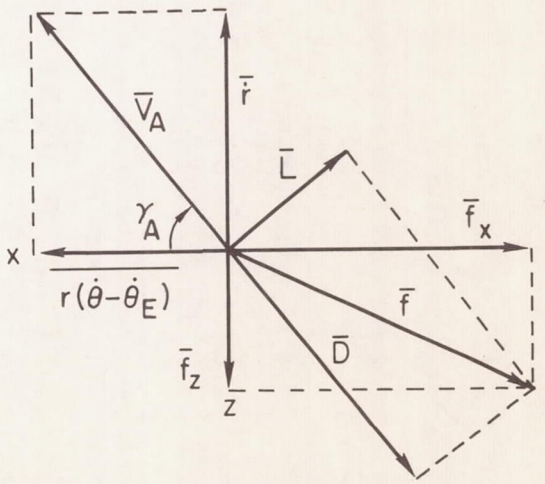

Relationship of flight-path angle to components of velocity and force.

Sketch (c)

Since equations (1) describe the motion of the vehicle, they may also be used by the on-board computer for the inertial navigation system. These equations are rewritten for the indicated trajectory using i subscripts for the indicated position, velocity, and force components.

$$\left.\begin{aligned} \ddot{r}_i - r_i\dot{\theta}_i^2 &= -\frac{\mu}{r_i^2} - f_{z_i} \\ r_i\ddot{\theta}_i + 2\dot{r}_i\dot{\theta}_i &= f_{x_i} \end{aligned}\right\} \qquad (5)$$

The indicated force components are those along the indicated horizontal and vertical of the measured accelerometer forces. The measured force components differ from the true values largely because of initial accelerometer misalinement, θ_{a_o}, gyro drift rate (which causes further accelerometer misalinement), $\dot{\theta}_a$, accelerometer biases, U_{x_a} and U_{z_a}, and accelerometer scale factor uncertainties, S_{x_a} and S_{z_a}. With the help of sketch (a) it can be seen that the measured force components given by the accelerometers may be determined for computing purposes by first resolving the actual force components through $-\theta$ into the inertial coordinate system, then resolving through θ_a into the accelerometer coordinate system, and then adding accelerometer biases and multiplying by accelerometer scale factors with their uncertainties. The indicated vertical and horizontal components are then obtained by resolving through θ_i. The components of actual force along the accelerometer axes, found by resolving through $-\theta$ and θ_a, are

$$\left.\begin{aligned} f_{x_a} &= f_x \cos(-\theta + \theta_{a_o} + \dot{\theta}_a t) + f_z \sin(-\theta + \theta_{a_o} + \dot{\theta}_a t) \\ f_{z_a} &= -f_x \sin(-\theta + \theta_{a_o} + \dot{\theta}_a t) + f_z \cos(-\theta + \theta_{a_o} + \dot{\theta}_a t) \end{aligned}\right\} \qquad (6)$$

The measured force components given by the accelerometer outputs are

$$\left.\begin{aligned} f_{x_{a(\text{measured})}} &= (f_{x_a} + gU_{x_a})SF_{x_a} \\ f_{z_{a(\text{measured})}} &= (f_{z_a} + gU_{z_a})SF_{z_a} \end{aligned}\right\} \qquad (7)$$

where

$$\left.\begin{aligned} SF_{x_a} &= 1 + S_{x_a} \\ SF_{z_a} &= 1 + S_{z_a} \end{aligned}\right\} \qquad (8)$$

When equations (6) and (8) are substituted into equations (7) and the measured force components are then resolved through θ_i, the indicated force components are found to be

$$
\left.
\begin{aligned}
f_{x_i} = {} & \cos\theta_i[f_x \cos(-\theta + \theta_{a_o} + \dot{\theta}_a t) \\
& + f_z \sin(-\theta + \theta_{a_o} + \dot{\theta}_a t) + gU_{x_a}](1 + S_{x_a}) \\
& + \sin\theta_i[-f_x \sin(-\theta + \theta_{a_o} + \dot{\theta}_a t) \\
& + f_z \cos(-\theta + \theta_{a_o} + \dot{\theta}_a t) + gU_{z_a}](1 + S_{z_a}) \\
f_{z_i} = {} & -\sin\theta_i[f_x \cos(-\theta + \theta_{a_o} + \dot{\theta}_a t) \\
& + f_z \sin(-\theta + \theta_{a_o} + \dot{\theta}_a t) + gU_{x_a}](1 + S_{x_a}) \\
& + \cos\theta_i[-f_x \sin(-\theta + \theta_{a_o} + \dot{\theta}_a t) \\
& + f_z \cos(-\theta + \theta_{a_o} + \dot{\theta}_a t) + gU_{z_a}](1 + S_{z_a})
\end{aligned}
\right\} \qquad (9)
$$

Position and velocity errors are computed by merely subtracting the actual components of position and velocity from the indicated components. This is illustrated in sketch (a) for position components. The equations are

$$
\left.
\begin{aligned}
r_e &= r_i - r = h_e = h_i - h \\
\theta_e &= \theta_i - \theta \\
\dot{r}_e &= \dot{r}_i - \dot{r} = \dot{h}_e = \dot{h}_i - \dot{h} \\
\dot{\theta}_e &= \dot{\theta}_i - \dot{\theta}
\end{aligned}
\right\} \qquad (10)
$$

These equations are used in this form for instantaneous and final errors. The initial errors and true values are usually specified and equations (10) are used to compute the initial indicated values.

Partial Derivative Equations for Linear Error Analysis

The requirements for a linear error analysis to be valid can be understood by examining the equations for the total differentials of the final position and velocity components. In equation (11) the total differential of final altitude is shown as an example.

$$
\begin{aligned}
dh_f = {} & \frac{\partial h_f}{\partial h_o} dh_o + \frac{\partial h_f}{\partial \theta_o} d\theta_o + \frac{\partial h_f}{\partial \dot{h}_o} d\dot{h}_o + \frac{\partial h_f}{\partial \dot{\theta}_o} d\dot{\theta}_o + \frac{\partial h_f}{\partial \theta_{a_o}} d\theta_{a_o} + \frac{\partial h_f}{\partial \dot{\theta}_a} d\dot{\theta}_a \\
& + \frac{\partial h_f}{\partial U_x} dU_x + \frac{\partial h_f}{\partial U_z} dU_z + \frac{\partial h_f}{\partial SF_x} dSF_x + \frac{\partial h_f}{\partial SF_z} dSF_z
\end{aligned} \qquad (11)
$$

A linear error analysis is valid provided the partial derivatives may be treated as constants when the differential quantities are replaced by incremental or error quantities as shown in equation (12).

$$h_{ef} = \frac{\partial h_f}{\partial h_o} h_{eo} + \frac{\partial h_f}{\partial \theta_o} \theta_{eo} + \frac{\partial h_f}{\partial \dot{h}_o} \dot{h}_{eo} + \frac{\partial h_f}{\partial \dot{\theta}_o} \dot{\theta}_{eo} + \frac{\partial h_f}{\partial \theta a_o} \theta a_o + \frac{\partial h_f}{\partial \dot{\theta}_a} \dot{\theta}_a$$
$$+ \frac{\partial h_f}{\partial U_x} U_x + \frac{\partial h_f}{\partial U_z} U_z + \frac{\partial h_f}{\partial SF_x} S_x + \frac{\partial h_f}{\partial SF_z} S_z \qquad (12)$$

Under these conditions a final altitude error, for example, would be directly proportional to any one of the initial condition or equipment errors, and the final altitude error due to several initial condition and equipment errors would be the superimposed sum of the final altitude errors due to each individual initial condition or equipment error taken separately.

For the range of initial error quantities for which a linear error analysis is valid, equations similar to equation (12) may be written for all of the final error quantities. In matrix form these equations appear as

$$\begin{bmatrix} h_{ef} \\ \theta_{ef} \\ \dot{h}_{ef} \\ \dot{\theta}_{ef} \end{bmatrix} = \begin{bmatrix} \frac{\partial h_f}{\partial h_o} & \frac{\partial h_f}{\partial \theta_o} & \frac{\partial h_f}{\partial \dot{h}_o} & \frac{\partial h_f}{\partial \dot{\theta}_o} & \frac{\partial h_f}{\partial \theta a_o} & \frac{\partial h_f}{\partial \dot{\theta}_a} & \frac{\partial h_f}{\partial U_x} & \frac{\partial h_f}{\partial U_z} & \frac{\partial h_f}{\partial SF_x} & \frac{\partial h_f}{\partial SF_z} \\ \frac{\partial \theta_f}{\partial h_o} & \frac{\partial \theta_f}{\partial \theta_o} & \frac{\partial \theta_f}{\partial \dot{h}_o} & \frac{\partial \theta_f}{\partial \dot{\theta}_o} & \frac{\partial \theta_f}{\partial \theta a_o} & \frac{\partial \theta_f}{\partial \dot{\theta}_a} & \frac{\partial \theta_f}{\partial U_x} & \frac{\partial \theta_f}{\partial U_z} & \frac{\partial \theta_f}{\partial SF_x} & \frac{\partial \theta_f}{\partial SF_z} \\ \frac{\partial \dot{h}_f}{\partial h_o} & \frac{\partial \dot{h}_f}{\partial \theta_o} & \frac{\partial \dot{h}_f}{\partial \dot{h}_o} & \frac{\partial \dot{h}_f}{\partial \dot{\theta}_o} & \frac{\partial \dot{h}_f}{\partial \theta a_o} & \frac{\partial \dot{h}_f}{\partial \dot{\theta}_a} & \frac{\partial \dot{h}_f}{\partial U_x} & \frac{\partial \dot{h}_f}{\partial U_z} & \frac{\partial \dot{h}_f}{\partial SF_x} & \frac{\partial \dot{h}_f}{\partial SF_z} \\ \frac{\partial \dot{\theta}_f}{\partial h_o} & \frac{\partial \dot{\theta}_f}{\partial \theta_o} & \frac{\partial \dot{\theta}_f}{\partial \dot{h}_o} & \frac{\partial \dot{\theta}_f}{\partial \dot{\theta}_o} & \frac{\partial \dot{\theta}_f}{\partial \theta a_o} & \frac{\partial \dot{\theta}_f}{\partial \dot{\theta}_a} & \frac{\partial \dot{\theta}_f}{\partial U_x} & \frac{\partial \dot{\theta}_f}{\partial U_z} & \frac{\partial \dot{\theta}_f}{\partial SF_x} & \frac{\partial \dot{\theta}_f}{\partial SF_z} \end{bmatrix} \begin{bmatrix} h_{eo} \\ \theta_{eo} \\ \dot{h}_{eo} \\ \dot{\theta}_{eo} \\ \theta a_o \\ \dot{\theta}_a \\ U_x \\ U_z \\ S_x \\ S_z \end{bmatrix} \qquad (13)$$

Once the partial derivatives are evaluated, the final errors can be determined as functions of the initial errors. From equation (13) it can be seen that one way to evaluate the partial derivatives would be to use only one initial condition or equipment error in each computer run, and to divide the final errors by the initial condition or equipment error used to obtain one column in the partial derivative matrix. For the initial condition and equipment errors being considered, then, ten separate runs are required to obtain the complete partial derivative matrix.

It is possible with matrix methods to calculate the partial derivative matrix by using ten runs which merely have independent sets of initial condition and equipment errors rather than only one error in each run. This process can be explained by writing equation (13) once for each of the ten independent sets of final errors that result from the ten independent sets of initial errors.

$$\left.\begin{aligned} [F_1] &= [P]\,[S_1] \\ [F_2] &= [P]\,[S_2] \\ &\cdot \quad\; \cdot \quad \cdot \\ &\cdot \quad\; \cdot \quad \cdot \\ &\cdot \quad\; \cdot \quad \cdot \\ [F_{10}] &= [P]\,[S_{10}] \end{aligned}\right\} \tag{14}$$

Equations (14) can be combined into

$$[F_1\ F_2\ \cdots\ F_{10}] = [P][S_1\ S_2\ \cdots\ S_{10}] \tag{15}$$

The partial derivative matrix may then be obtained by post multiplying the final error matrix by the inverse initial error matrix

$$[P] = [F_1\ F_2\ \cdots\ F_{10}][S_1\ S_2\ \cdots\ S_{10}]^{-1} \tag{16}$$

It should be apparent that for a particular trajectory, the errors which exist at any instant of time may be considered to be the initial errors which cause the resulting final errors at any later instant of time. Once the instantaneous errors for ten runs, with each run having completely independent sets of errors, have been obtained along a particular trajectory, then the ten sets of errors at any point in time may be considered to be the initial or start errors for the ten sets of errors at any later point in time. With equation (16), then, the data from the ten runs are sufficient to calculate the partial derivative matrix which relates the initial errors at any point in time to the final errors at some later point in time. This process has been used in the present study to calculate the partial derivative matrix between the final time, t_f', which is always taken at the nominal 30 km final altitude, and every preceding start time along the trajectory.

Trajectory Parameters and Vehicle Characteristics

The trajectories considered deviated slightly from a typical circumlunar trajectory and are described below in two phases: a space phase, which is largely independent of vehicle characteristics, and a reentry phase, which is very dependent upon vehicle characteristics. The atmosphere density, ρ, for the reentry phase was obtained from reference 4. Both phases used earth constants of $\mu = 3.986135\times10^5$ km^3/sec^2, $r_E = 6{,}397.14$ km, and $\dot{\theta}_E = 7.292115\times10^{-5}$ radian/sec.

The typical circumlunar trajectory representing the primary example for the space phase has the following approximate elliptical parameters:

$$\left.\begin{aligned} a &= 2.025\times10^5 \text{ km} \\ e &= 0.9683 \\ r_p &= 6.423\times10^3 \text{ km} \\ H &= 7.099\times10^4 \text{ km}^2/\text{sec} \end{aligned}\right\} \tag{17}$$

For an actual reentry vehicle, especially one with a pilot, it may be desirable to have completed the alinement of the inertial platform and to have put precise initial conditions into the system (i.e., to have started the system) as much as an hour before reentry in order to have time to establish confidence in the system operation and to avoid last minute pilot procedures. To use available trajectory data it was necessary to choose a start time of 63.51 minutes before reentry as the earliest time to be considered. For the typical lunar trajectory considered the initial conditions at this start time were:

$$\left.\begin{aligned} t_o &= 0 \\ t_o' &= -63.51 \text{ min} \\ h_o &= 18{,}476.30 \text{ km} \\ r_E\dot{\theta}_o &= -12{,}010.33 \text{ km} \\ \dot{h}_o &= -4.68508 \text{ km/sec} \\ r_E\dot{\theta}_o &= 0.7329312 \text{ km/sec} \end{aligned}\right\} \qquad (18)$$

The resulting values for γ_{A_o} and V_{A_o} were

$$\left.\begin{aligned} \gamma_{A_o} &= -77.4414^\circ \\ V_{A_o} &= 4.79992 \text{ km/sec} \end{aligned}\right\} \qquad (19)$$

For easy interpretation of range values, a reference of $\theta = 0$ for $t' = 0$ has been chosen at the reentry altitude of 121.92 km, or 400,000 ft.

The reentry phase is very dependent upon the vehicle characteristics. For the vehicle considered $C_DA/m = 4.1\times10^{-9}$ km^2/kg (or mg/C_DA = 50.1 lb/ft^2) and $(L/D)_{max} = \pm0.5$. Constant and variable L/D trajectories were examined. For the variable L/D trajectories $L/D = -3.281\,\dot{h}$ for $0 < L/D < (L/D)_{max}$ (obtained from ref. 5). The constant L/D trajectories were obtained for values of L/D from 0.05 to 0.27, and the variable L/D trajectories were obtained by changing the reentry flight-path angle (at 121.92 km) from -6.4795° to -5.8629° and varying L/D as just described. These represent a wide variety of reentry trajectories, since the constant L/D entries have very high decelerations and the variable L/D entries have rather low decelerations.

The specific trajectories considered are shown in figure 1, and some of their more important parameters are shown in table I. The longest trajectory considered has a range of about three-fourths of the circumference of the earth (earth circumference $\approx$ 40,000 km) and the final time after reentry is about 1 hour. The medium length trajectories, having reentry times near 20 minutes, are more desirable from the standpoint of reentry time. Trajectory 4, which has a medium range, low peak deceleration, and low skip altitude, will be emphasized in the remainder of this report to illustrate the principles being discussed. Time histories of the trajectory variables are given in figure 2 for trajectory 4. Curves for altitude, range, altitude rate, and range rate are shown in figure 2(a), and the corresponding curves for velocity, flight-path angle, and force per unit mass are shown in figure 2(b).

Initial Condition and Equipment Errors

It is highly desirable to use a currently realistic set of values for typical initial condition and equipment errors. Consequently, the following initial condition errors were obtained from the results of a study of a midcourse navigation system for a circumlunar mission.

$$\left.\begin{aligned} h_{e_o} &= 5 \text{ km} \\ r_o\theta_{e_o} &= 0.5 \text{ km} \\ \dot{h}_{e_o} &= 5\times10^{-4} \text{ km/sec} \\ r_o\dot{\theta}_{e_o} &= 2\times10^{-5} \text{ km/sec} \end{aligned}\right\} \qquad (20)$$

The correctness of the order of magnitude of these errors may be verified by referring to the standard case in figure 4 of reference 6. These initial condition errors are roughly an order of magnitude larger than those present in radio tracking data, provided the radio tracking system has been allowed sufficient tracking time for filtering and smoothing its data.

The following conservative equipment errors were used as independent discrete values in this study without regard to statistical variations:

$$\left.\begin{aligned} \theta_{a_o} &= 2\times10^{-4} \text{ radian} \cong 40 \text{ seconds of arc} \\ \dot{\theta}_a &= 1\times10^{-6} \text{ radian/sec} \cong 13 \text{ meru} \\ U_{x_a} &= U_{z_a} = 1\times10^{-4} \text{ g} \\ S_{x_a} &= S_{z_a} = 1\times10^{-4} \text{ g/g} \end{aligned}\right\} \qquad (21)$$

RESULTS AND DISCUSSION

The navigation errors in position and velocity during reentry into the earth's atmosphere were analyzed to establish the range of initial condition and equipment errors over which a linear analysis is valid, that is, to establish the range over which the partial derivatives of final position and velocity with respect to initial conditions and equipment parameters may be treated as constants. The results of this analysis were then used to demonstrate the use of partial derivatives for estimating the final errors that result from various combinations of initial condition and equipment errors with the inertial navigation process started at various times before reentry.

The results establishing the region of validity of a linear error analysis will be presented as follows: First, the relationship between the final and instantaneous errors will be illustrated using trajectory 4 as an example. Then the final errors will be given for each of the seven trajectories in figure 1 so that the validity of a linear error analysis can be examined for the magnitude of

errors given in equations (20) and (21). Finally, trajectory 4 will be used as an example to demonstrate the range of linearity of final errors with respect to initial condition and equipment errors.

The results of using partial derivatives for estimating final errors will be presented as follows: Trajectory 4 will be used to present data for curves of partial derivatives of final errors with respect to initial condition and equipment errors as functions of start time. These curves will then be multiplied by initial condition and equipment errors as functions of start time to give curves of final errors versus start time. The relative effects of initial condition and equipment errors resulting from starting the system operating at various times before reentry will be examined, and ways of reducing the resulting errors will be discussed.

Range of Linearity

For trajectory 4 the time histories of errors in altitude, range angle, altitude rate, and range angle rate are shown in figure 3(a), and corresponding errors in velocity and flight-path angle are shown in figure 3(b). For these curves all of the errors in equations (20) and (21) were used as the initial condition and equipment errors. In figure 3(a) it is seen that the errors change slowly and remain small for the first 30 minutes and then begin to change more rapidly and to become large. The changing nature of these errors can be explained if one considers the different behavior of inertial navigation errors, in general, above and below circular velocity (ref. 7). It is known that when $r\dot{\theta}$ has been reduced below the required velocity for circular orbit at that altitude, the altitude error, which is the most significant error, becomes unstable and results in large errors after reentry is completed. This instability is not entirely obvious for the medium range trajectory of figure 3, but it is rather pronounced for longer range trajectories. It should be noted in figure 3(a) that the altitude error as shown remains positive at all times; however, different combinations of positive and negative initial condition and equipment errors could have caused the altitude error to be more oscillatory in nature and to become negative during part or all of the time.

The final errors in figure 3 exist where the error curves terminate. From table I it is seen that the final time after reentry, t_f, is 23.69 minutes, and this occurs when the "actual" final altitude, h_f, is 26.75 km. This value was used instead of exactly 30 km (the nominal value) because it was the nearest time available from the computer data after 30 km had been reached.

The final errors which result from applying each of the initial condition and equipment errors of equations (20) and (21) to each of the seven trajectories illustrated in figure 1 are shown in tables II(a) through (g). The results from 11 computer runs are shown in each table. For runs 1 through 10 the final errors are shown which result from just the initial condition, I.C., or equipment, Equip., error indicated for each run with all other initial condition and equipment errors set equal to zero. For example, in table II(d) for trajectory 4, computer run 1, with an initial altitude error of 5 km and all other initial condition and equipment errors set equal to zero, resulted in a final altitude error of 6.65 km

and a final range error of -19.54 km. The only other significant errors in this table resulted from gyro drift rate and accelerometer biases (runs 6, 7, and 8). When a linear error analysis is valid, the estimated value of the superimposed effects of all the initial condition and equipment errors may be obtained as the algebraic sum for initial condition and equipment errors. The estimated values of 9.79 km for altitude and -36.93 km for range may be compared with the results of run 11, where all of the initial condition and equipment errors were used. For run 11 the final errors of 9.71 for altitude and -37.03 for range compare very well with the estimated final errors given as the algebraic sum for initial condition and equipment errors. Hence, superposition of the errors is valid here, indicating that a linear error analysis is valid for the assumed errors. Similar results for the other six trajectories are shown in the other parts of table II.

The worst possible condition would exist if all final errors had the same sign. When the absolute magnitudes of the final errors in table II(d) are summed, the resulting errors of 62.56 km for altitude and 72.75 km for range are seen to be very large. These large errors are caused mostly by equipment, as shown by the values of 54.72 km for altitude and 51.34 km for range due to equipment errors only.

The absolute magnitudes of the final errors for all seven trajectories are summarized in table III. When these are plotted as functions of final range, the curves shown in figure 4 are obtained. From these curves it is apparent that the errors for high deceleration trajectories, illustrated by the constant L/D curves, are somewhat larger than for the low deceleration trajectories, illustrated by the variable L/D curves. From figure 4(a) it is also apparent that the final range errors increase continuously with increases in final range. From figure 4(b), however, it is seen that some of the curves for final altitude errors reach maximum values and then decrease as the final range increases. From this figure it can be seen that equipment errors, rather than the initial condition errors, are causing the decreasing final altitude errors. Although a satisfactory explanation of this decrease in final altitude errors is not known to the authors, a study of longer range trajectories not included in this report has shown that final attitude errors reach a minimum value for a final range slightly greater than the longest ranges illustrated and then generally increase with further increases in final range.

Since a linear error analysis appears to be valid for the errors in equations (20) and (21), it is not surprising to find that the final errors in table IV(a) for negative initial condition and equipment errors are the negatives of those in table II(d) for positive initial condition and equipment errors of the same magnitude. Furthermore, when initial condition and equipment errors which are ten times larger than those in equations (20) and (21) are used, a linear error analysis still appears to give approximately correct results, as shown in table IV(b). In this table the algebraic sums of final errors in runs 1 through 10 agree fairly well with the final errors in run 11. Furthermore, a comparison with table II(d) shows that the final errors (as well as the initial condition and equipment errors) in table IV(b) are approximately ten times the corresponding final errors in table II(d).

When initial condition and equipment errors 100 times as large as those in equations (20) and (21) are used, however, a linear error analysis is no longer valid, as shown in table IV(c).

Although trajectory 4 has been used as an example in table IV, very similar results are obtained for any of the seven representative trajectories in figure 1.

The range of errors for which a linear error analysis is valid can be more clearly demonstrated if the final errors are plotted versus initial condition and equipment errors. Again using trajectory 4 as an example, the ranges of linearity for initial altitude errors and initial range errors are shown in parts (a) and (b), respectively, of figure 5. Final altitude error is used here as an example. The solid lines show the actual curves obtained and the broken lines show the linear results. It is readily apparent that the initial altitude error of 5 km and the initial range error of 0.5 km given in equation (20) are well within the linear range of values. In fact, initial errors ten times these values are still well within the linear range. Additional data, not included in this report, have shown that the range of linearity for all of the initial condition and equipment errors extends beyond ten times the values in equations (20) and (21). The errors chosen in equations (20) and (21) are conservative, so that errors larger than ten times these values are unrealistic for sophisticated space applications. Hence, it is concluded that a linear error analysis for realistic reentry conditions will usually be valid.

Use of Partial Derivatives for Estimating Final Errors

Now that the range of linearity has been demonstrated to include conservative errors for realistic reentry conditions, the use of the partial derivatives for estimating the effects of starting the inertial navigation process at various times before reentry will be demonstrated. Curves of partial derivatives versus start time, obtained as outlined under the section entitled "Partial Derivative Equations for Linear Error Analysis," will first be presented. With trajectory 4 as an example a set of these partial derivative curves is given in figures 6 through 9. As would be expected, the partial derivative of each final quantity with respect to its initial value is equal to unity at the final time, and the partial derivative of each final quantity with respect to every other initial quantity is equal to zero at the final time. Most of the partial derivatives decrease continuously to the final values of 0 or 1. Several of them change signs, and some of them have abrupt changes when the atmosphere is reached.

As the start time is delayed, the partial derivatives with respect to altitude increase, which means that if an identical initial altitude error were used (with the other errors remaining zero), regardless of the start time, then smaller final errors would result if the inertial navigation process were started well before the atmosphere is reached, rather than just immediately before the atmosphere is reached. In fact, the worst possible time to start with an altitude error only would be just before the atmosphere is reached, since most of the partial derivatives with respect to altitude peak in this vicinity. Although this interesting result is contrary to the fairly common assumption made in inertial navigation that the smallest final errors would occur if the start time is delayed until the latest possible moment, it can be partially explained theoretically if elliptical equations for a nonatmospheric reentry are used and a perfect inertial navigation system is assumed. When the equations of motion given by equation (1) with $f_x = f_y = 0$ (for no atmosphere) are used, the vehicle follows an elliptic trajectory in which radius of perigee is analogous to final altitude.

The partial derivative of radius of perigee with respect to initial radius (or altitude) has the shape shown in figure 10(a).[2] Comparison of this curve with the the curve for the partial derivative of final altitude with respect to initial altitude in figure 6(a) shows that the curves have similar shapes. Figure 10(b) shows some similarity to the partial derivative of final altitude with respect to initial altitude rate shown in figure 6(a), and figure 10(c) shows very close similarity to the partial derivative of final altitude with respect to initial range angle rate shown in figure 6(a). The partial derivative of radius of perigee with respect to initial range angle is zero, since the trajectory is merely shifted through a small angle around the earth. However, as shown in figure 6(a), the partial derivative of final altitude with respect to initial range angle is not zero (although it is small enough to contribute only a very small final altitude error), since an error in range angle causes a misalinement of the indicated and actual horizontal and vertical axes so that the inertial navigation system computes the wrong value of deceleration.

It is interesting to note that the start time for the maximum values of the partial derivatives with respect to initial altitude varies depending upon the particular choice of independent variables. When V_A and γ_A are used as independent variables instead of $\dot{h}$ and $\dot{\theta}$, the curves shown in figures 11(a), (b), and (c) are obtained for the partial derivative of radius of perigee with respect to initial radius, velocity, and flight-path angle. The curve in figure 11(a) does not reach a peak before the atmosphere is reached, as does the corresponding curve in figure 10(a), although it does increase in magnitude as the atmosphere is approached (ref. 8). This difference in the curves of the partial derivatives of radius of perigee with respect to initial radius does not imply that the use of different coordinate systems would result in different answers. The results for the two coordinate systems would be the same since, if one assumes statistically uncorrelated errors in one coordinate system, the coordinate transformation will give correlated errors in the other coordinate system. The curves of figures 10 and 11 assume uncorrelated errors in each coordinate system.

For an actual inertial navigation system being used on a vehicle, no one knows what the error correlation will be; however, it would seem desirable to avoid any situation which might produce large errors. Since the effects of an initial altitude error by itself may be rather large, as previously illustrated, it would be wise to consider the possibility of reducing the effects of the initial altitude error by putting the initial conditions into the system and starting its operation at some time prior to that for which the partial derivatives with respect to initial altitude reach maximum values.

The partial derivative curves shown in figures 6 and 7 will now be used to estimate the position errors which result from starting the inertial navigation process at different times before reentry. The estimation procedure will be illustrated graphically. For illustration it will be assumed that the initial condition and equipment errors in equations (20) and (21) are those at any start time of the inertial navigation process, regardless of the initial time or altitude. When the errors in equations (20) and (21) are multiplied by the appropriate partial derivatives at each start time in figures 6 and 7, the final errors shown by the solid lines in figures 12(a) and (b) are obtained. The final errors for initial range angle error, initial altitude rate error, initial range angle

[2]The equations for figures 10 and 11 are derived in the appendix.

rate error, initial misalinement angle, and accelerometer scale factor uncertainties are too small to be shown. Hence, for the assumed errors the only significant equipment errors are gyro drift rate and accelerometer biases. The sum of the absolute final altitude error for all initial condition errors is approximately equal to the final error for initial altitude error only. The broken-line curves in figure 12(a) represent the sum of the absolute values of final altitude errors for equipment errors only and for initial condition and equipment errors combined. It is significant that the final altitude errors due to equipment errors decrease as the atmosphere is approached, while the final altitude errors due to initial condition errors increase as the atmosphere is approached. From figure 12(a) (top curve) it can be seen that it would be desirable, from an altitude error standpoint, to start the inertial navigation system between 20 and 30 minutes before reentry.

To illustrate the accuracy of this estimation process, a set of estimated final errors will be compared with a set of computed final errors at the particular start time of 3.58 minutes before reentry. The estimated errors obtained by multiplying the partial derivatives by the initial condition and equipment errors are shown in part (a) of table V. The computed errors obtained from 10 separate computer runs started at 3.58 minutes before reentry are shown in part (b) of table V. Most of the values in the two tables agree very well with each other but some of the values for accelerometer biases do not. As shown in figures 6(b), 7(b), 8(b), and 9(b), the partial derivatives with respect to U_x and U_z become quite small at $t'_o = -3.58$ minutes. Because of this, the partial derivatives were determined with insufficient accuracy, which accounts for the discrepancies between tables V(a) and V(b) for the errors in accelerometer biases.

Some consideration will now be given to the magnitude of the final errors obtained. From figure 12 it is apparent that the final errors for combined initial condition and equipment errors are fairly large, especially when it is considered that the final altitude error is somewhat larger than the actual final altitude of about 30 km and the final range error is much larger than the value of several kilometers desired for convenient recovery of the vehicle. Although trajectory 4 has been used as an example, figure 4 shows that the errors for this trajectory are the same order of magnitude as the errors that would be expected for any other reasonable trajectory.

It should be emphasized that the results presented in figure 12 are based on the main assumption that the initial condition and equipment errors are the same for any altitude before reentry. The same procedure may be used to estimate the starting time effects for initial condition and equipment errors which change as a function of altitude. Depending on the method used for obtaining the initial conditions, the errors may or may not be significantly smaller near reentry than an hour before reentry. From the example illustrated in figure 12 it is apparent that if the initial altitude error is several times smaller near reentry than an hour before reentry, the final errors in altitude and range will be reduced by starting the inertial navigation system at a time less than about 20 minutes before reentry.

When the inertial navigation process is started about an hour before reentry, the final errors result predominantly from equipment errors, rather than initial

condition errors. Accelerometer bias and gyro drift are the chief contributors. Using the outputs of the accelerometers as zero above the atmosphere, so that the biases are not integrated prior to reentry, can greatly reduce the effects of accelerometer bias. The final errors for trajectory 4, calculated with initial condition and equipment errors of equations (20) and (21) but with accelerometer outputs of zero above the atmosphere, are shown in table VI. Comparison of this table with table II(d) shows that leaving the accelerometers off above the atmosphere produced much smaller errors due to accelerometer bias, but did not significantly affect the other individual final errors. Hence the sum of absolute values for equipment errors and the sum of the absolute values for initial condition and equipment errors are reduced correspondingly. Thus, leaving the accelerometers off above the atmosphere helps to reduce the final errors.

CONCLUDING REMARKS

The final errors in position and velocity when an inertial navigation system is used during reentry into the earth's atmosphere have been analyzed for a given set of initial condition and equipment errors. The analysis has shown that for realistic errors and reentry conditions a linear error analysis will usually be valid; that is, the partial derivatives of final position and velocity with respect to initial conditions and equipment parameters may be treated as constants. Also, the analysis has demonstrated that these partial derivatives can be used to estimate the final errors which result from using various combinations of initial condition and equipment errors with the inertial navigation process started at various times before reentry.

Some interesting error relationships were revealed by the analysis of a specific reentry from a lunar trajectory. When the inertial navigation process is started just prior to reentry, the final errors resulting from initial condition errors predominate, but when the process is started well before reentry those from equipment errors predominate. Altitude error is the most significant initial condition error, and accelerometer bias and gyro drift are the most significant equipment errors. The final errors due to accelerometer bias may be greatly reduced by treating the outputs of the accelerometers as zero above the atmosphere.

Although a specific reentry trajectory terminating a flight path from the moon has been used to a large extent in this report, sufficient consideration has been given to other trajectories to indicate that these error relationships should also exist for any realistic reentry trajectory.

Ames Research Center
National Aeronautics and Space Administration
Moffett Field, Calif., Feb. 21, 1963

APPENDIX

DERIVATION OF PARTIAL DERIVATIVES FOR AN ELLIPSE

The general shapes of the partial derivative curves shown in figure 6(a) can be partially explained if elliptical equations of a nonatmospheric reentry are used and a perfect inertial navigation system is assumed. For these conditions, differences between indicated and actual elliptical trajectories will result from initial condition errors only. For such comparisons the radius of perigee is analogous to final altitude and partial derivatives of radius of perigee are analogous to partial derivatives of final altitude. Good analogies for the partial derivatives of final range, final altitude rate, and final range rate are much more difficult to obtain and will not be considered.

It should be noted that the partial derivatives of radius of perigee are only analogous to the partial derivatives of final altitude, and they differ in several respects. The most obvious differences result from the absence of atmosphere and the assumption of a perfect inertial navigation system. A less obvious difference is that the partial derivatives of final altitude are found by taking the difference between the indicated and actual altitude at some particular final time, whereas the partial derivatives of radius of perigee are calculated as the difference in radii of perigee for the actual and indicated elliptical trajectories. This difference is not thought to be too significant, however, since the elliptical paths are nearly parallel to the earth's surface and to each other in the vicinity of the radius of perigee and since the time between the starting point and the radius of perigee is nearly the same for the two elliptical trajectories.

To obtain the appropriate partial derivatives, it is desired to find equations for r_p in terms of both the r, θ, $\dot{r}$, and $\dot{\theta}$ and the r, θ, V, and γ systems. For simplicity the derivation of r_p will be made in terms of the r, θ, V, and γ system, and the equation in the r, θ, $\dot{r}$, and $\dot{\theta}$ system will then be found merely by substituting the relationships

$$\left.\begin{aligned} V^2 &= \dot{r}^2 + r^2\dot{\theta}^2 \\ V\cos\gamma &= r\dot{\theta} \end{aligned}\right\} \qquad (22)$$

which are illustrated in sketch (d). It should be observed that sketch (d) differs slightly from sketch (c) because the rotation of the earth is not considered in the calculation of V and γ.

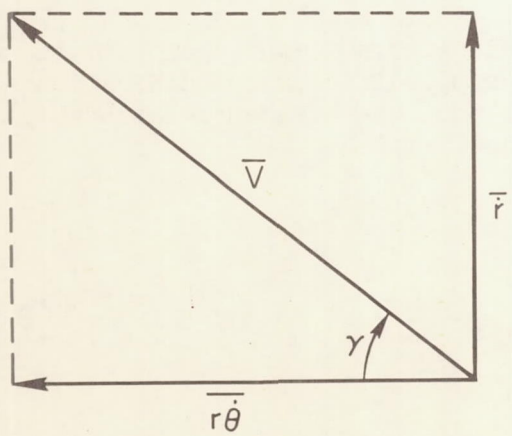

Sketch (d)

The equations for an orbit described by an ellipse are well known. The following equation for r_p will be used as a starting point in the present derivation (ref. 2, p. 24).

$$r_p = \frac{r}{2 - (rV^2/\mu)}\left[1 - \sqrt{1 - \frac{rV^2 \cos^2\gamma}{\mu}\left(2 - \frac{rV^2}{\mu}\right)}\right] \tag{23}$$

This equation may be differentiated explicitly in this form to obtain the partial derivatives of r_p with respect to r, V, and γ, but the results are difficult to simplify because of the presence of the radical. A simpler approach is first to remove the radical by transferring everything except the radical to the left side of the equation and then squaring both sides of the equation to obtain:

$$1 - 2\frac{r_p}{r}\left(2 - \frac{rV^2}{\mu}\right) + \frac{r_p^2}{r^2}\left(2 - \frac{rV^2}{\mu}\right)^2 = 1 - \frac{rV^2 \cos^2\gamma}{\mu}\left(2 - \frac{rV^2}{\mu}\right) \tag{24}$$

Now, subtracting 1 from each side of this equation, then multiplying both sides by $\mu r^2/[2 - (rV^2/\mu)]$, and then transposing everything to the left side of the equation gives:

$$-2\mu r_p r + r^3V^2 \cos^2\gamma + r_p^2(2\mu - rV^2) = 0 \tag{25}$$

This equation is now in a simple form for implicit differentiation, and equations (22) may be used to rewrite it in terms of r, $\dot{r}$, and $\dot{\theta}$

$$-2\mu r_p r + r^5\dot{\theta}^2 + r_p^2[2\mu - r(\dot{r}^2 + r^2\dot{\theta}^2)] = 0 \tag{26}$$

When equation (26) is differentiated implicitly, the following partial derivatives of r_p with respect to r, $\dot{r}$, and $\dot{\theta}$ are obtained:

$$\left.\begin{aligned}
\frac{\partial r_p}{\partial r} &= \frac{2\mu r_p - 5r^4\dot{\theta}^2 + r_p^2(\dot{r}^2 + 3r^2\dot{\theta}^2)}{-2\mu r + 2r_p[2\mu - r(\dot{r}^2 + r^2\dot{\theta}^2)]} \\
\frac{\partial r_p}{\partial \dot{r}} &= \frac{r_p^2 r\dot{r}}{-\mu r + r_p[2\mu - r(\dot{r}^2 + r^2\dot{\theta}^2)]} \\
\frac{\partial r_p}{\partial \dot{\theta}} &= \frac{-r^5\dot{\theta} + r_p^2 r^3\dot{\theta}}{-\mu r + r_p[2\mu - r(\dot{r}^2 + r^2\dot{\theta}^2)]}
\end{aligned}\right\} \tag{27}$$

Similarly from equation (25) the following partials of r_p with respect to r, V, and γ are obtained:

$$\left.\begin{aligned}
\frac{\partial r_p}{\partial r} &= \frac{2\mu r_p - 3r^2V^2 \cos^2\gamma + r_p^2V^2}{-2\mu r + 2r_p(2\mu - rV^2)} \\
\frac{\partial r_p}{\partial V} &= \frac{-r^3V \cos^2\gamma + r_p^2 rV}{-\mu r + r_p(2\mu - rV^2)} \\
\frac{\partial r_p}{\partial \gamma} &= \frac{r^3V^2 \cos\gamma \sin\gamma}{-\mu r + r_p(2\mu - rV^2)}
\end{aligned}\right\} \tag{28}$$

For both systems the partial derivative of r_p with respect to θ is zero, since r_p is independent of θ as shown by equation (23). It should also be immediately recognized that the partial derivative of r_p with respect to r is different in equations (27) and (28), since different quantities have been assumed to remain constant during the differentiation processes.

To obtain plots of these partial derivatives versus time, several other equations are required. Time is obtained by using Kepler's equation, which can be written as

$$t_p = E - e \sin(E) \tag{29}$$

where t_p is the time to perigee and E is the eccentric anomaly, given by

$$E = \cos^{-1} \frac{a - r}{ae} \tag{30}$$

The time at radius, r, on the ellipse can be obtained in terms of time after reentry, t', by subtracting t_p at r from t_p at an altitude of 121.92 km. The other equations needed for an elliptical trajectory in addition to equations (22) and (27) through (30) are:

$$\left.\begin{aligned} V^2 &= \mu \left(\frac{2}{r} - \frac{1}{a}\right) \\ H &= rV \cos \gamma = r^2\dot{\theta} = \text{constant} \end{aligned}\right\} \tag{31}$$

Now, there are sufficient equations to obtain the plots shown in figures 10 and 11 using the values for a, e, and H in equations (17).

REFERENCES

1. White, John S.: Investigation of the Errors of an Inertial Guidance System During Satellite Re-entry. NASA TN D-322, 1960.

2. Jensen, Jorgen, et al.: Design Guide to Orbital Flight. McGraw-Hill Book Co., Inc., 1962.

3. Pitman, George R., Jr., ed.: Inertial Guidance. John Wiley and Sons, Inc., 1962.

4. Minzer, Raymond A., Champion, K. S. W., and Pond, H. L.: The ARDC Model Atmosphere. TR 59-267, Air Force Cambridge Research Center, Aug. 1959.

5. Wingrove, Rodney C.: A Study of Guidance to Reference Trajectories for Lifting Reentry at Supercircular Velocity. NASA TR R-151, 1963.

6. McLean, John D., Schmidt, Stanley F., and McGee, Leonard A.: Optimal Filtering and Linear Prediction Applied to a Midcourse Navigation System for the Circumlunar Mission. NASA TN D-1208, 1962.

7. Young, Laurence R.: Inertial Navigation in an Orbital Vehicle. M. S. Thesis, MIT, 1959.

8. Wong, Thomas J., and Slye, Robert E.: The Effect of Lift on Entry Corridor Depth and Guidance Requirements for the Return Lunar Flight. NASA TR R-80, 1961.

TABLE I.- DATA FOR TRAJECTORIES SHOWN IN FIGURE 1

Trajectory	1	2	3	4	5	6	7
Final range, $r_E\theta_f$, km	1,510	3,130	7,330	9,780	16,940	20,980	27,830
Final time, t_f', min	3.87	9.13	18.17	23.69	39.83	47.81	67.17
Final altitude (nominal 30 km), h_f, km	27.62	29.50	26.51	26.75	29.57	28.31	26.22
L/D	.05	-3.281 $\dot{h}$	.22	-3.281 $\dot{h}$	.25	-3.281 $\dot{h}$	.27
Peak deceleration, g	9.45	4.37	6.59	2.93	6.31	2.97	6.13
γ_{A_o}, deg	-77.4414	-77.4414	-77.4414	-77.4070	-77.4414	-77.4068	-77.4414
γ_{AR}, deg	-6.4795	-6.4795	-6.4795	-5.8860	-6.4795	-5.8629	-6.4795
V_{A_o}, km/sec	4.79992	4.79992	4.79992	4.79992	4.79992	4.79992	4.79992
V_{AR}, km/sec	10.51436	10.51436	10.51436	10.51383	10.51436	10.51515	10.51436

Note: Except for changes in γ_{A_o} for the variable L/D trajectories, the initial conditions in equations (18) and (19) were used.

TABLE II.- FINAL ERRORS RESULTING FROM ERRORS ASSUMED IN EQUATIONS (20) AND (21)

(a) For trajectory 1

Run	Errors assumed	Final errors: Altitude, h_{e_f}, km	Range, $r_E\theta_{e_f}$, km	Altitude rate, $\dot{h}_{e_f}$, 10^{-3} km/sec	Range rate, $r_E\dot{\theta}_{e_f}$, 10^{-3} km/sec
1	Initial condition errors: h_{e_o} = 5.0 km	6.13	-14.61	14.2	-3.34
2	$r_o\theta_{e_o}$ = 0.5 km	-.02	.13	-.21	.01
3	$\dot{h}_{e_o}$ = 5.0x10^{-4} km/sec	.44	-2.92	1.91	-.21
4	$r_o\dot{\theta}_{e_o}$ = 2.0x10^{-5} km/sec	.10	-.10	.14	-.08
5	Equipment errors: θ_{a_o} = 2.0x10^{-4} radian	-.21	0	-2.04	-.08
6	$\dot{\theta}_a$ = 1.0x10^{-6} radian/sec	-4.08	-.06	-39.99	-1.44
7	U_{x_a} = 1.0x10^{-4} g	9.97	-8.58	15.24	-8.04
8	U_{z_a} = 1.0x10^{-4} g	.10	8.93	-2.92	1.25
9	S_{x_a} = 1.0x10^{-4} g/g	.05	-.03	.49	-.30
10	S_{z_a} = 1.0x10^{-4} g/g	-.05	-.07	-.45	-.69
[a]Σ	(Runs 1 through 10)	12.43	-17.31	-13.63	-12.92
[b]Σ	|Runs 1 through 4|	6.69	17.76	16.46	3.64
[c]Σ	|Runs 5 through 10|	14.46	17.67	61.13	31.89
[d]Σ	|Runs 1 through 10|	21.15	35.43	77.59	35.53
11	Final errors from all initial condition and equipment errors	12.42	-17.30	-13.64	-13.01

[a]Algebraic sum of final errors from initial condition and equipment errors
[b]Sum of absolute values of final errors from initial condition errors
[c]Sum of absolute values of final errors from equipment errors
[d]Sum of absolute values of final errors from initial condition and equipment errors

TABLE II.- FINAL ERRORS RESULTING FROM ERRORS ASSUMED IN EQUATIONS (20) AND (21) - Continued

Run	Errors assumed	Final errors: Altitude, h_{e_f}, km	Range, $r_E\theta_{e_f}$, km	Altitude rate, $\dot{h}_{e_f}$, 10^{-3} km/sec	Range rate, $r_E\dot{\theta}_{e_f}$, 10^{-3} km/sec
(b) For trajectory 2					
1	Initial condition errors: h_{e_o} = 5.0 km	8.02	-16.37	19.01	-0.10
2	Initial condition errors: $r_o\theta_{e_o}$ = 0.5 km	-.06	.13	-.24	-.01
3	Initial condition errors: $\dot{h}_{e_o}$ = 5.0×10^{-4} km/sec	-.46	2.91	2.15	.64
4	Initial condition errors: $r_o\dot{\theta}_{e_o}$ = 2.0×10^{-5} km/sec	.13	-.14	.22	-.06
5	Equipment errors: θ_{a_o} = 2.0×10^{-4} radian	-.62	.04	-2.34	-.08
6	Equipment errors: $\dot{\theta}_a$ = 1.0×10^{-6} radian/sec	-12.29	.76	-47.31	-1.93
7	Equipment errors: U_{x_a} = 1.0×10^{-4} g	13.68	-13.23	23.36	-7.53
8	Equipment errors: U_{z_a} = 1.0×10^{-4} g	1.28	8.60	-1.44	-2.02
9	Equipment errors: S_{x_a} = 1.0×10^{-4} g/g	.14	-.14	.60	-.56
10	Equipment errors: S_{z_a} = 1.0×10^{-4} g/g	-.16	-.14	-.56	-.37
[a]Σ	(Runs 1 through 10)	10.58	-23.40	-6.55	-12.02
[b]Σ	|Runs 1 through 4|	8.67	19.55	21.62	.81
[c]Σ	|Runs 5 through 10|	28.17	22.91	75.61	12.49
[d]Σ	|Runs 1 through 10|	36.84	42.46	97.23	13.30
11	Final errors from all initial condition and equipment errors	10.56	-23.39	-6.56	-12.13
(c) For trajectory 3					
1	Initial condition errors: h_{e_o} = 5.0 km	8.29	-20.21	24.96	1.15
2	Initial condition errors: $r_o\theta_{e_o}$ = 0.5 km	-.11	.19	-.30	.04
3	Initial condition errors: $\dot{h}_{e_o}$ = 5.0×10^{-4} km/sec	-.15	-2.42	1.93	1.30
4	Initial condition errors: $r_o\dot{\theta}_{e_o}$ = 2.0×10^{-5} km/sec	.15	-.25	.33	-.06
5	Equipment errors: θ_{a_o} = 2.0×10^{-4} radian	-1.07	.57	-2.97	.37
6	Equipment errors: $\dot{\theta}_a$ = 1.0×10^{-6} radian/sec	-21.58	11.02	-63.64	6.15
7	Equipment errors: U_{x_a} = 1.0×10^{-4} g	17.30	-25.80	35.24	-8.45
8	Equipment errors: U_{z_a} = 1.0×10^{-4} g	6.38	4.10	4.94	-6.88
9	Equipment errors: S_{x_a} = 1.0×10^{-4} g/g	.11	-.31	.26	-.81
10	Equipment errors: S_{z_a} = 1.0×10^{-4} g/g	-.38	.04	-.60	.16
[a]Σ	(Runs 1 through 10)	8.94	-33.07	.15	-7.03
[b]Σ	|Runs 1 through 4|	8.7	23.07	27.52	2.55
[c]Σ	|Runs 5 through 10|	46.82	41.85	107.65	22.82
[d]Σ	|Runs 1 through 10|	55.52	64.92	135.17	25.37
11	Final errors from all initial condition and equipment errors	8.92	-33.13	.18	-7.33

[a]Algebraic sum of final errors from initial condition and equipment errors
[b]Sum of absolute values of final errors from initial condition errors
[c]Sum of absolute values of final errors from equipment errors
[d]Sum of absolute values of final errors from initial condition and equipment errors

TABLE II.- FINAL ERRORS RESULTING FROM ERRORS ASSUMED IN EQUATIONS (20) AND (21) - Continued

Run	Errors assumed		Final errors: Altitude, h_{e_f}, km	Range, $r_{E\theta_{e_f}}$, km	Altitude rate, $\dot{h}_{e_f}$, 10^{-3} km/sec	Range rate, $r_E\dot{\theta}_{e_f}$, 10^{-3} km/sec
(d) For trajectory 4						
1	Initial condition errors	h_{e_o} = 5.0 km	6.65	-19.54	23.47	5.02
2		$r_o\theta_{e_o}$ = 0.5 km	-.11	.21	-.30	.02
3		$\dot{h}_{e_o}$ = 5.0x10^{-4} km/sec	-.93	-1.43	.52	1.89
4		$r_E\dot{\theta}_{e_o}$ = 2.0x10^{-5} km/sec	.15	-.23	.36	0
5	Equipment errors	θ_{a_o} = 2.0x10^{-4} radian	-1.12	.85	-2.99	.17
6		$\dot{\theta}_a$ = 1.0x10^{-6} radian/sec	-23.68	16.63	-67.21	1.59
7		U_{x_a} = 1.0x10^{-4} g	17.77	-31.18	39.72	-3.14
8		U_{z_a} = 1.0x10^{-4} g	11.60	-2.14	14.52	-9.84
9		S_{x_a} = 1.0x10^{-4} g/g	-.02	-.32	-.15	-.60
10		S_{z_a} = 1.0x10^{-4} g/g	-.52	.22	-.62	.17
[a]Σ (Runs 1 through 10)			9.79	-36.93	7.32	-4.72
[b]Σ |Runs 1 through 4|			7.84	21.41	24.65	6.93
[c]Σ |Runs 5 through 10|			54.72	51.34	125.22	15.51
[d]Σ |Runs 1 through 10|			62.56	72.75	149.87	22.44
11	Final errors from all initial condition and equipment errors		9.71	-37.03	7.31	-5.04
(e) For trajectory 5						
1	Initial condition errors	h_{e_o} = 5.0 km	12.20	-29.64	38.82	.64
2		$r_o\theta_{e_o}$ = 0.5 km	-.17	.42	-.47	.03
3		$\dot{h}_{e_o}$ = 5.0x10^{-4} km/sec	-.33	-.15	1.00	.89
4		$r_o\dot{\theta}_{e_o}$ = 2.0x10^{-5} km/sec	.18	-.48	.55	.01
5	Equipment errors	θ_{a_o} = 2.0x10^{-4} radian	-1.65	2.87	-4.71	.32
6		$\dot{\theta}_a$ = 1.0x10^{-6} radian/sec	-34.30	55.52	-107.00	3.88
7		U_{x_a} = 1.0x10^{-4} g	17.24	-52.70	55.29	1.59
8		U_{z_a} = 1.0x10^{-4} g	15.55	-22.96	27.31	-10.48
9		S_{x_a} = 1.0x10^{-4} g/g	-.19	-.17	-.10	.21
10		S_{z_a} = 1.0x10^{-4} g/g	-1.09	1.37	-2.00	-.04
[a]Σ (Runs 1 through 10)			7.44	-45.92	8.69	-2.95
[b]Σ |Runs 1 through 4|			12.88	30.69	40.84	1.57
[c]Σ |Runs 5 through 10|			70.02	135.59	196.42	16.52
[d]Σ |Runs 1 through 10|			82.90	166.28	237.26	18.09
11	Final errors from all initial condition and equipment errors		7.23	-46.10	8.78	-3.85

[a]Algebraic sum of final errors from initial condition and equipment errors
[b]Sum of absolute values of final errors from initial condition errors
[c]Sum of absolute values of final errors from equipment errors
[d]Sum of absolute values of final errors from initial condition and equipment errors

TABLE II.- FINAL ERRORS RESULTING FROM ERRORS ASSUMED IN EQUATIONS (20) AND (21) - Concluded

Run	Errors assumed	Final errors: Altitude, h_{e_f}, km	Range, $r_E\theta_{e_f}$, km	Altitude rate, $\dot{h}_{e_f}$, 10^{-3} km/sec	Range rate, $r_E\dot{\theta}_{e_f}$, 10^{-3} km/sec
(f) For trajectory 6					
1	Initial condition errors: h_{e_o} = 5.0 km	7.00	-18.79	27.36	4.83
2	Initial condition errors: $r_o\theta_{e_o}$ = 0.5 km	-.07	.31	-.32	-.08
3	Initial condition errors: $\dot{h}_{e_o}$ = 5.0×10^{-4} km/sec	-1.40	2.67	-2.40	.43
4	Initial condition errors: $r_o\dot{\theta}_{e_o}$ = 2.0×10^{-5} km/sec	.13	-.38	.49	.10
5	Equipment errors: θ_{a_o} = 2.0×10^{-4} radian	-.66	1.76	-3.16	-.83
6	Equipment errors: $\dot{\theta}_a$ = 1.0×10^{-6} radian/sec	-16.77	33.90	-81.47	-20.30
7	Equipment errors: U_{x_a} = 1.0×10^{-4} g	8.73	-40.98	44.12	14.36
8	Equipment errors: U_{z_a} = 1.0×10^{-4} g	19.97	-38.96	44.76	-3.57
9	Equipment errors: S_{x_a} = 1.0×10^{-4} g/g	-.28	.18	-.06	.03
10	Equipment errors: S_{z_a} = 1.0×10^{-4} g/g	-1.47	2.15	-3.34	-.10
[a]Σ (Runs 1 through 10)		15.18	-58.14	25.98	-5.13
[b]Σ |Runs 1 through 4|		8.6	22.15	30.57	5.44
[c]Σ |Runs 5 through 10|		47.88	117.93	176.92	39.19
[d]Σ |Runs 1 through 10|		56.48	140.08	207.49	44.63
11	Final errors from all initial condition and equipment errors	14.90	-57.94	25.63	-5.64
(g) For trajectory 7					
1	Initial condition errors: h_{e_o} = 5.0 km	21.35	-51.06	66.07	2.44
2	Initial condition errors: $r_o\theta_{e_o}$ = 0.5 km	-.13	.55	-.62	-.13
3	Initial condition errors: $\dot{h}_{e_o}$ = 5.0×10^{-4} km/sec	1.44	-1.10	2.44	-1.11
4	Initial condition errors: $r_o\dot{\theta}_{e_o}$ = 2.0×10^{-5} km/sec	.23	-.66	.84	.10
5	Equipment errors: θ_{a_o} = 2.0×10^{-4} radian	-1.29	4.23	-6.24	-1.32
6	Equipment errors: $\dot{\theta}_a$ = 1.0×10^{-6} radian/sec	-30.03	80.92	-150.10	-30.39
7	Equipment errors: U_{x_a} = 1.0×10^{-4} g	11.55	-53.88	65.83	18.13
8	Equipment errors: U_{z_a} = 1.0×10^{-4} g	8.19	-44.15	41.57	11.09
9	Equipment errors: S_{x_a} = 1.0×10^{-4} g/g	-.56	.72	-1.06	-.46
10	Equipment errors: S_{z_a} = 1.0×10^{-4} g/g	-1.29	3.54	-3.89	-.25
[a]Σ (Runs 1 through 10)		9.46	-60.89	14.84	-1.90
[b]Σ |Runs 1 through 4|		23.15	53.37	69.97	3.78
[c]Σ |Runs 5 through 10|		52.90	187.44	268.69	61.64
[d]Σ |Runs 1 through 10|		76.05	240.81	338.66	65.42
11	Final errors from all initial condition and equipment errors	9.12	-60.53	14.59	-3.60

[a]Algebraic sum of final errors from initial condition and equipment errors
[b]Sum of absolute values of final errors from initial condition errors
[c]Sum of absolute values of final errors from equipment errors
[d]Sum of absolute values of final errors from initial condition and equipment errors

TABLE III.- SUMMARY OF MAXIMUM POSSIBLE ERRORS; THE SUM OF ABSOLUTE VALUES OF FINAL ERRORS FROM TABLE II

Trajectory	Final time, t_f', min	Final range, $10^3 r_{E\theta_f}$, km	Sum of absolute values of final errors from -					
			Initial condition errors		Equipment errors		Initial condition and equipment errors	
			Altitude, km	Range, km	Altitude, km	Range, km	Altitude, km	Range, km
1	3.87	1.51	6.69	17.76	14.46	17.67	21.15	35.43
2	9.13	3.13	8.67	19.55	28.17	22.91	36.84	42.46
3	18.17	7.33	8.70	23.07	46.82	41.85	55.52	64.92
4	23.69	9.78	7.84	21.41	54.72	51.34	62.56	72.75
5	39.83	16.94	12.88	30.69	70.02	135.59	82.90	166.28
6	47.81	20.98	8.60	22.15	47.88	117.93	56.48	140.08
7	67.17	27.83	23.15	53.37	52.90	187.44	76.05	240.81

TABLE IV.- FINAL ERRORS FOR TRAJECTORY 4 WITH VARIOUS INITIAL ERRORS

(a) Initial errors which are negatives of those in equations (20) and (21)						
Run	Errors assumed		Final errors			
			Altitude, h_{e_f}, km	Range, $r_{E\theta_{e_f}}$, km	Altitude rate, $\dot{h}_{e_f}$, 10^{-3} km/sec	Range rate, $r_{E\dot{\theta}_{e_f}}$, 10^{-3} km/sec
1	Initial condition errors	$h_{e_o} = -5.0$ km	-6.61	19.54	-23.45	-4.99
2		$r_o\theta_{e_o} = -0.5$ km	.11	-.21	.30	-.02
3		$\dot{h}_{e_o} = -5.0\times10^{-4}$ km/sec	.93	1.43	-.52	-1.89
4		$r_o\dot{\theta}_{e_o} = -2.0\times10^{-5}$ km/sec	-.15	.29	-.36	0
5	Equipment errors	$\theta_{a_o} = -2.0\times10^{-4}$ radian	1.12	-.85	2.99	-.17
6		$\dot{\theta}_a = -1.0\times10^{-6}$ radian/sec	23.77	-16.50	67.18	-1.22
7		$U_{x_a} = -1.0\times10^{-4}$ g	-17.73	31.28	-39.81	3.27
8		$U_{z_a} = -1.0\times10^{-4}$ g	-11.59	2.14	-14.52	9.89
9		$S_{x_a} = -1.0\times10^{-4}$ g/g	.02	.32	.15	.60
10		$S_{z_a} = -1.0\times10^{-4}$ g/g	.52	-.22	.62	-.17
[a]	Σ (Runs 1 through 10)		-9.61	37.22	-7.42	5.3
[b]	$\Sigma \lvert$ Runs 1 through 4 $\rvert$		7.8	21.47	24.63	6.9
[c]	$\Sigma \lvert$ Runs 5 through 10 $\rvert$		54.76	51.31	125.28	15.32
[d]	$\Sigma \lvert$ Runs 1 through 10 $\rvert$		62.56	72.78	149.91	22.22
11	Final errors from all initial condition and equipment errors		-9.68	37.15	-7.41	4.98

[a] Algebraic sum of final errors from initial condition and equipment errors
[b] Sum of absolute values of final errors from initial condition errors
[c] Sum of absolute values of final errors from equipment errors
[d] Sum of absolute values of final errors from initial condition and equipment errors

TABLE IV.- FINAL ERRORS FOR TRAJECTORY 4 WITH VARIOUS INITIAL ERRORS - Concluded

Run	Errors assumed	Final errors: Altitude, h_{e_f}, km	Range, $r_E\theta_{e_f}$, km	Altitude rate, $\dot{h}_{e_f}$, 10^{-3} km/sec	Range rate, $r_E\dot{\theta}_{e_f}$, 10^{-3} km/sec
(b) Initial errors ten times those in equations (20) and (21)					
1	Initial condition errors: h_{e_o} = 5.0x10 km	67.99	-195.35	235.38	51.24
2	Initial condition errors: $r_o\theta_{e_o}$ = 5.0 km	-1.12	2.14	-3.01	.17
3	Initial condition errors: $\dot{h}_{e_o}$ = 5.0x10^{-3} km/sec	-9.27	-14.34	5.27	19.01
4	Initial condition errors: $r_o\dot{\theta}_{e_o}$ = 2.0x10^{-4} km/sec	1.53	-2.85	3.64	-.02
5	Equipment errors: θ_{a_o} = 2.0x10^{-3} radian	-11.16	8.53	-29.90	1.77
6	Equipment errors: $\dot{\theta}_a$ = 1.0x10^{-5} radian/sec	-232.54	172.13	-672.71	33.68
7	Equipment errors: U_{x_a} = 1.0x10^{-3} g	179.30	-306.92	392.98	-26.12
8	Equipment errors: U_{z_a} = 1.0x10^{-3} g	116.41	-21.21	144.60	-95.98
9	Equipment errors: S_{x_a} = 1.0x10^{-3} g/g	-.22	-3.20	-1.50	-6.03
10	Equipment errors: S_{z_a} = 1.0x10^{-3} g/g	-5.25	2.21	-6.24	1.75
[a]Σ (Runs 1 through 10)		105.67	-316.44	68.51	-20.53
[b]Σ |Runs 1 through 4|		79.91	214.68	247.30	70.44
[c]Σ |Runs 5 through 10|		544.88	514.20	1247.94	165.33
[d]Σ |Runs 1 through 10|		624.79	728.80	1495.24	235.77
11	Final errors from all initial condition and equipment errors	98.45	-364.58	68.49	-52.63
(c) Initial errors one hundred times those in equations (20) and (21)					
1	Initial condition errors: h_{e_o} = 5.0x10^2 km	801.61	-1915.36	2328.24	588.21
2	Initial condition errors: $r_o\theta_{e_o}$ = 5.0x10 km	-11.23	21.41	-30.08	1.77
3	Initial condition errors: $\dot{h}_{e_o}$ = 5.0x10^{-2} km/sec	-86.24	-149.89	63.87	193.49
4	Initial condition errors: $r_o\dot{\theta}_{e_o}$ = 2.0x10^{-3} km/sec	15.36	-28.47	36.40	-.15
5	Equipment errors: θ_{a_o} = 2.0x10^{-2} radian	-110.50	86.55	-298.82	21.09
6	Equipment errors: $\dot{\theta}_a$ = 1.0x10^{-4} radian/sec	-1658.57	2232.62	-5692.00	3004.98
7	Equipment errors: U_{x_a} = 1.0x10^{-2} g	1886.10	-2618.51	3431.10	39.48
8	Equipment errors: U_{z_a} = 1.0x10^{-2} g	1197.35	-193.67	1387.22	-756.42
9	Equipment errors: S_{x_a} = 1.0x10^{-2} g/g	-2.17	-32.02	-14.67	-60.42
10	Equipment errors: S_{z_a} = 1.0x10^{-2} g/g	-52.58	22.34	-62.99	17.71
[a]Σ (Runs 1 through 10)		1979.13	-2575.00	1148.27	3049.74
[b]Σ |Runs 1 through 4|		914.43	2115.13	2458.59	783.62
[c]Σ |Runs 5 through 10|		4907.27	5185.71	10886.80	3900.10
[d]Σ |Runs 1 through 10|		5821.71	7300.84	13345.39	4683.72
11	Final errors from all initial condition and equipment errors	1080.58	-3035.27	199.06	-618.11

[a]Algebraic sum of final errors from initial condition and equipment errors
[b]Sum of absolute values of final errors from initial condition errors
[c]Sum of absolute values of final errors from equipment errors
[d]Sum of absolute values of final errors from initial condition and equipment errors

TABLE V.- FINAL ERRORS FOR TRAJECTORY 4 WITH START TIME OF 3.58 MINUTES BEFORE REENTRY

Run	Errors assumed	Final errors: Altitude, h_{e_f}, km	Range, $r_E\theta_{e_f}$, km	Altitude rate, $\dot{h}_{e_f}$, 10^{-3} km/sec	Range rate, $r_E\dot{\theta}_{e_f}$, 10^{-3} km/sec
(a) Estimated from partial derivatives					
1	Initial condition errors: h_{e_o} = 5.0 km	35.50	-26.34	63.40	-14.45
2	Initial condition errors: $r_o\theta_{e_o}$ = 0.5 km	-.40	.76	-1.07	.06
3	Initial condition errors: $\dot{h}_{e_o}$ = 5.0×10^{-4} km/sec	.46	-.93	.99	-.20
4	Initial condition errors: $r_o\dot{\theta}_{e_o}$ = 2.0×10^{-5} km/sec	.06	-.03	.10	-.03
5	Equipment errors: θ_{a_o} = 2.0×10^{-4} radian	-1.12	.85	-2.99	.17
6	Equipment errors: $\dot{\theta}_a$ = 1.0×10^{-6} radian/sec	-3.66	1.37	-13.63	-1.53
7	Equipment errors: U_{x_a} = 1.0×10^{-4} g	-.01	-1.09	-.13	-.84
8	Equipment errors: U_{z_a} = 1.0×10^{-4} g	2.05	-.81	3.97	-1.10
9	Equipment errors: S_{x_a} = 1.0×10^{-4} g/g	-.02	-.32	-.15	-.60
10	Equipment errors: S_{z_a} = 1.0×10^{-4} g/g	-.52	.22	-.62	.17
[a]Σ (Runs 1 through 10)		32.34	-26.32	49.87	-18.35
[b]Σ |Runs 1 through 4|		36.42	28.06	65.56	14.74
[c]Σ |Runs 5 through 10|		7.38	4.66	21.49	4.41
[d]Σ |Runs 1 through 10|		43.80	32.72	87.05	19.15
(b) Obtained from computer runs					
1	Initial condition errors: h_{e_o} = 5.0 km	36.11	-26.82	64.93	-14.70
2	Initial condition errors: $r_o\theta_{e_o}$ = 0.5 km	-.40	.77	-1.07	.06
3	Initial condition errors: $\dot{h}_{e_o}$ = 5.0×10^{-4} km/sec	.45	-.92	.97	-.19
4	Initial condition errors: $r_o\dot{\theta}_{e_o}$ = 2.0×10^{-5} km/sec	.06	-.03	.10	-.03
5	Equipment errors: θ_{a_o} = 2.0×10^{-4} radian	-1.12	.86	-2.99	.17
6	Equipment errors: $\dot{\theta}_a$ = 1.0×10^{-6} radian/sec	-3.71	1.32	-13.64	-1.70
7	Equipment errors: U_{x_a} = 1.0×10^{-4} g	2.00	-.82	3.88	-1.13
8	Equipment errors: U_{z_a} = 1.0×10^{-4} g	.02	1.17	.07	.89
9	Equipment errors: S_{x_a} = 1.0×10^{-4} g/g	-.51	.23	-.60	.15
10	Equipment errors: S_{z_a} = 1.0×10^{-4} g/g	-.04	-.32	-.18	-.58
[a]Σ (Runs 1 through 10)		32.86	-24.57	53.61	-17.06
[b]Σ |Runs 1 through 4|		37.02	28.54	67.07	14.98
[c]Σ |Runs 5 through 10|		7.40	4.72	21.36	4.62
[d]Σ |Runs 1 through 10|		44.42	33.26	88.43	19.60

[a]Algebraic sum of final errors from initial condition and equipment errors
[b]Sum of absolute values of final errors from initial condition errors
[c]Sum of absolute values of final errors from equipment errors
[d]Sum of absolute values of final errors from initial condition and equipment errors

TABLE VI.- FINAL ERRORS FOR TRAJECTORY 4 WITH ZERO OUTPUT FROM ACCELEROMETERS ABOVE ATMOSPHERE

Run	Errors assumed		Final errors			
			Altitude, h_{e_f}, km	Range, $r_E\theta_{e_f}$, km	Altitude rate, $\dot{h}_{e_f}$, 10^{-3} km/sec	Range rate, $r_E\dot{\theta}_{e_f}$, 10^{-3} km/sec
1	Initial condition errors	$h_{e_o} = 5.0$ km	6.70	-19.53	23.56	2.41
2		$r_o\theta_{e_o} = 0.5$ km	-.05	.23	-.21	-.01
3		$\dot{h}_{e_o} = 5.0\times10^{-4}$ km/sec	-.88	-1.41	.61	1.87
4		$r_o\dot{\theta}_{e_o} = 2.0\times10^{-5}$ km/sec	.21	-.27	.46	-.03
5	Equipment errors	$\theta_{a_o} = 2.0\times10^{-4}$ radian	-1.06	.87	-2.90	.15
6		$\dot{\theta}_a = 1.0\times10^{-6}$ radian/sec	-23.62	16.65	-67.12	.16
7		$U_{x_a} = 1.0\times10^{-4}$ g	-.04	-.82	-.18	-.87
8		$U_{z_a} = 1.0\times10^{-4}$ g	1.45	-.47	2.93	-.80
9		$S_{x_a} = 1.0\times10^{-4}$ g/g	.04	-.31	-.06	-.63
10		$S_{z_a} = 1.0\times10^{-4}$ g/g	-.46	.24	-.53	.15
[a]Σ (Runs 1 through 10)			-17.71	-4.82	-43.44	2.40
[b]Σ |Runs 1 through 4|			7.84	21.44	24.84	4.32
[c]Σ |Runs 5 through 10|			26.67	19.36	73.72	2.76
[d]Σ |Runs 1 through 10|			34.51	40.80	98.56	7.08
11	Final errors from all initial condition and equipment errors		-18.29	-5.00	-44.29	6.50

[a]Algebraic sum of final errors from initial condition and equipment errors
[b]Sum of absolute values of final errors from initial condition errors
[c]Sum of absolute values of final errors from equipment errors
[d]Sum of absolute values of final errors from initial condition and equipment errors

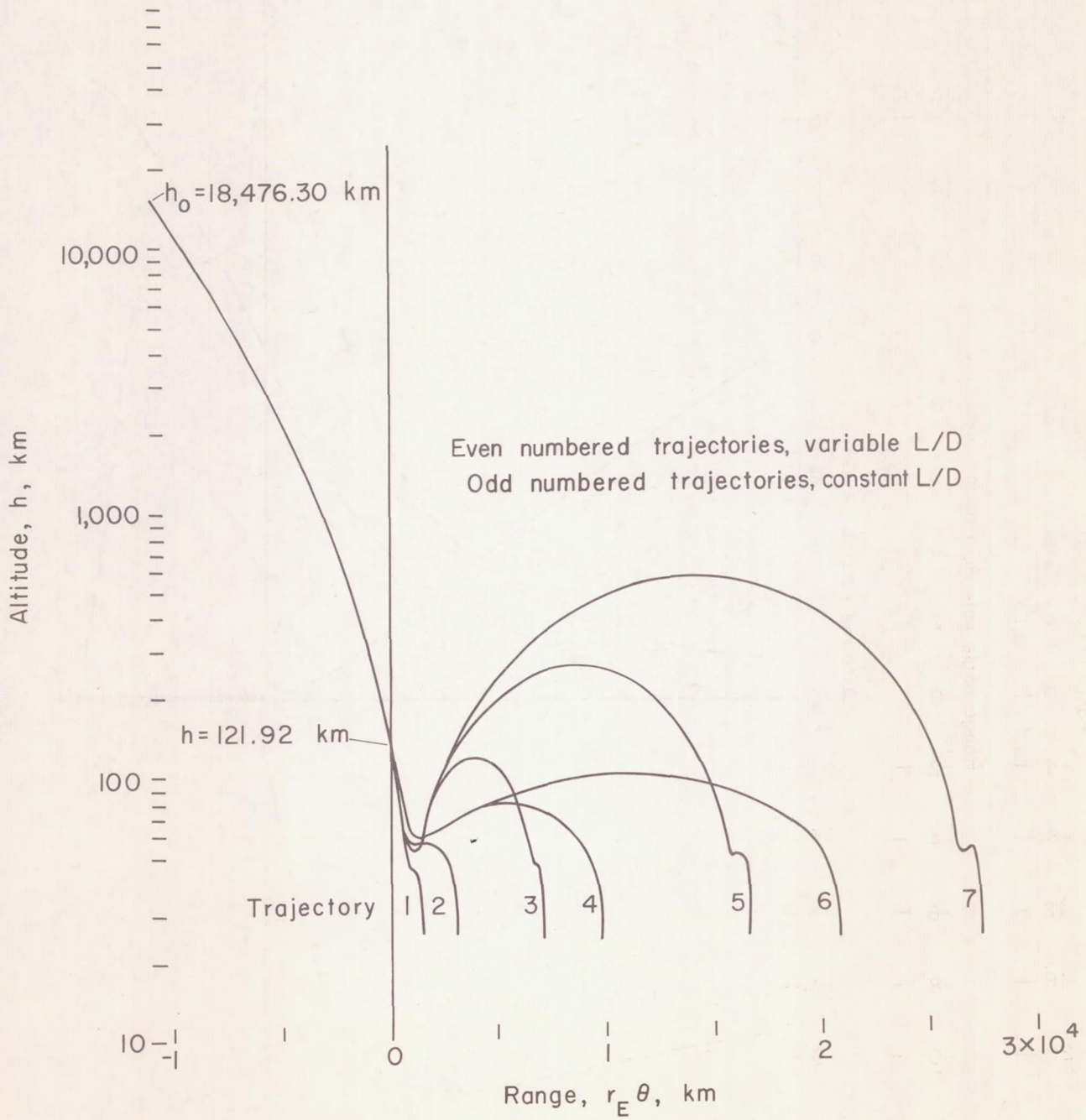

Figure 1.- Altitude versus range for typical constant and variable L/D trajectories.

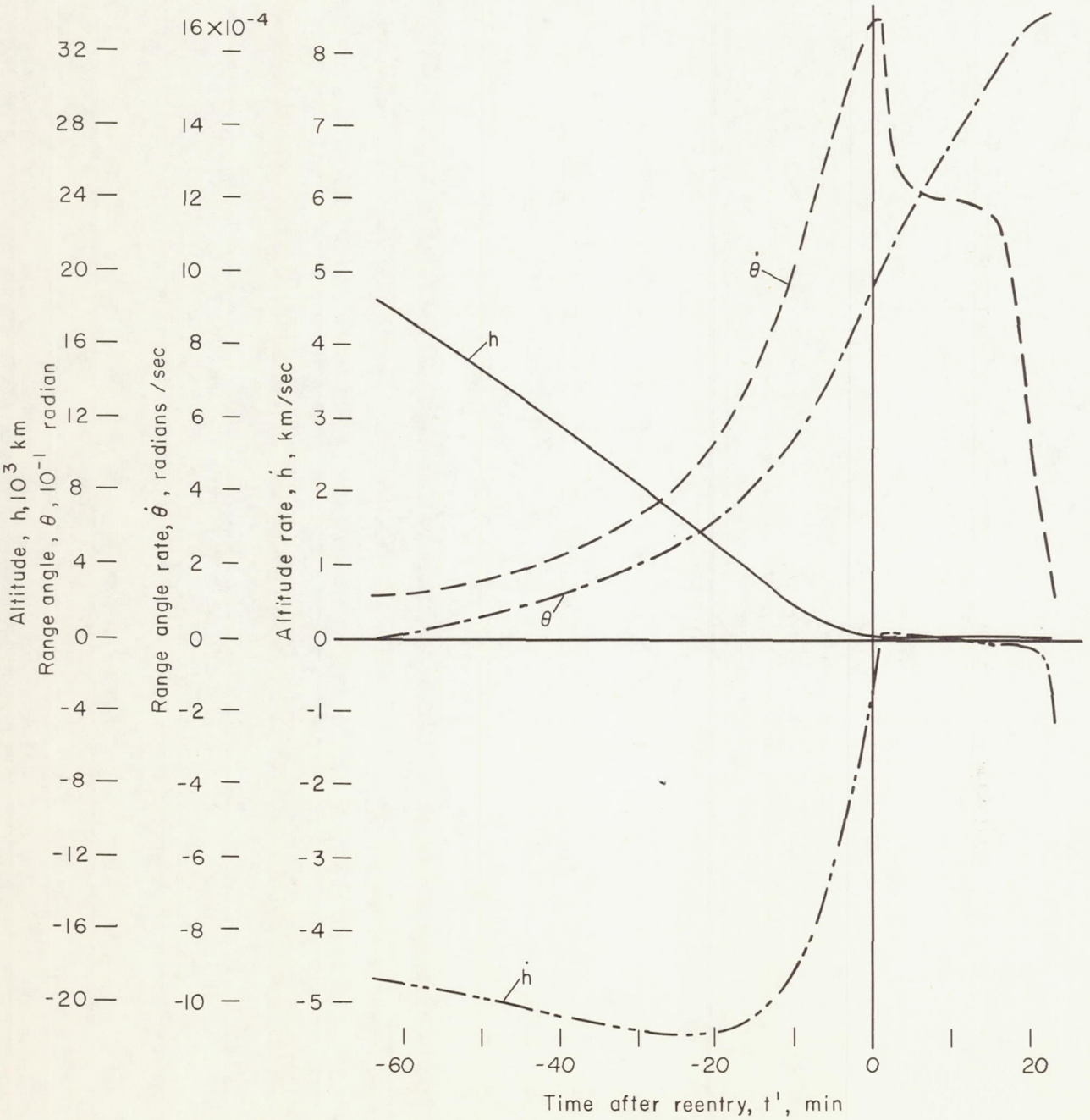

(a) Altitude, range angle, altitude rate, and range-angle rate.

Figure 2.- Time histories of trajectory variables for trajectory 4.

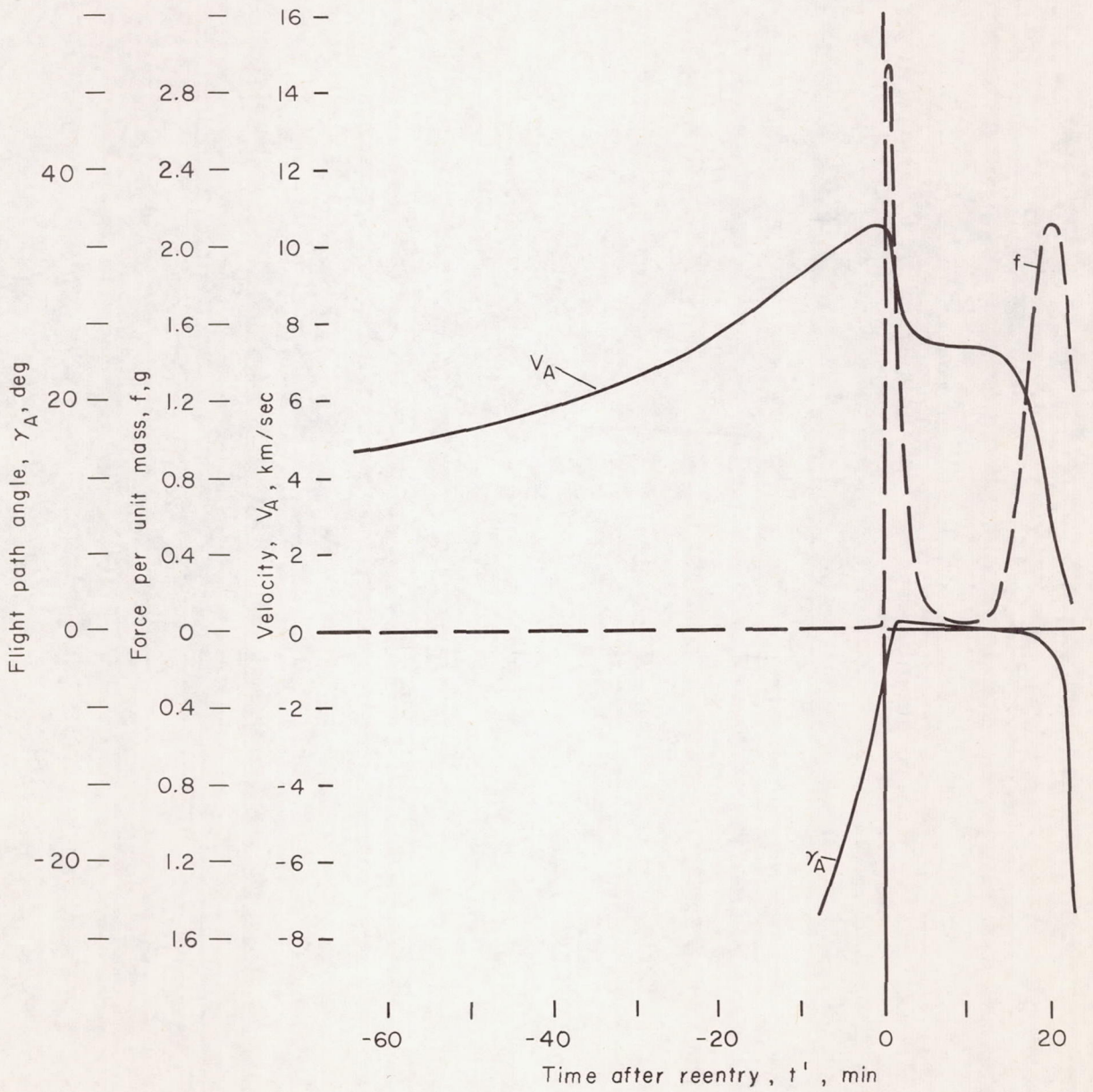

(b) Velocity, flight-path angle, and force per unit mass.

Figure 2.- Concluded.

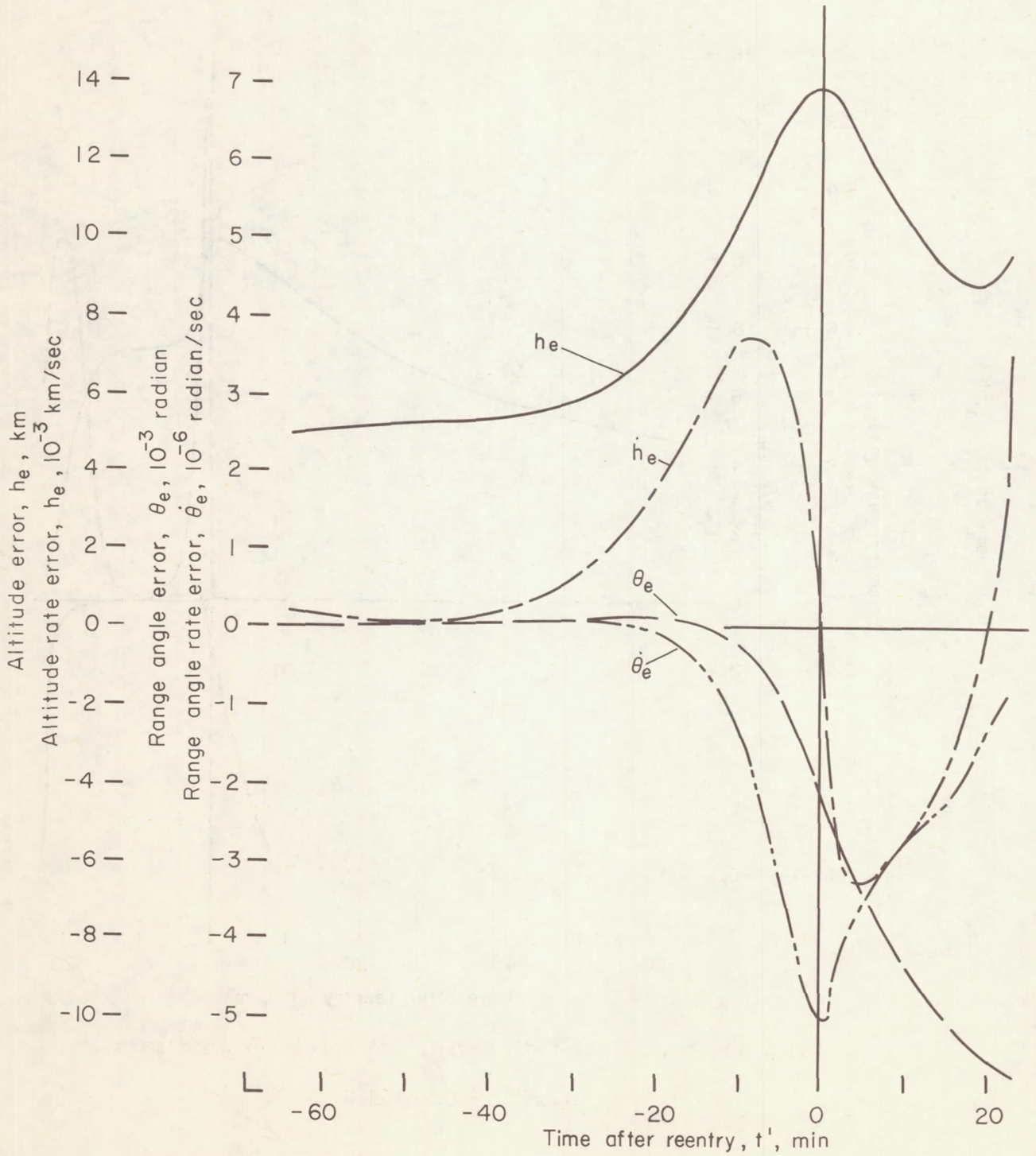

(a) Altitude, range angle, altitude rate, and range angle rate errors.

Figure 3.- Time histories of the errors in trajectory variables for trajectory 4.

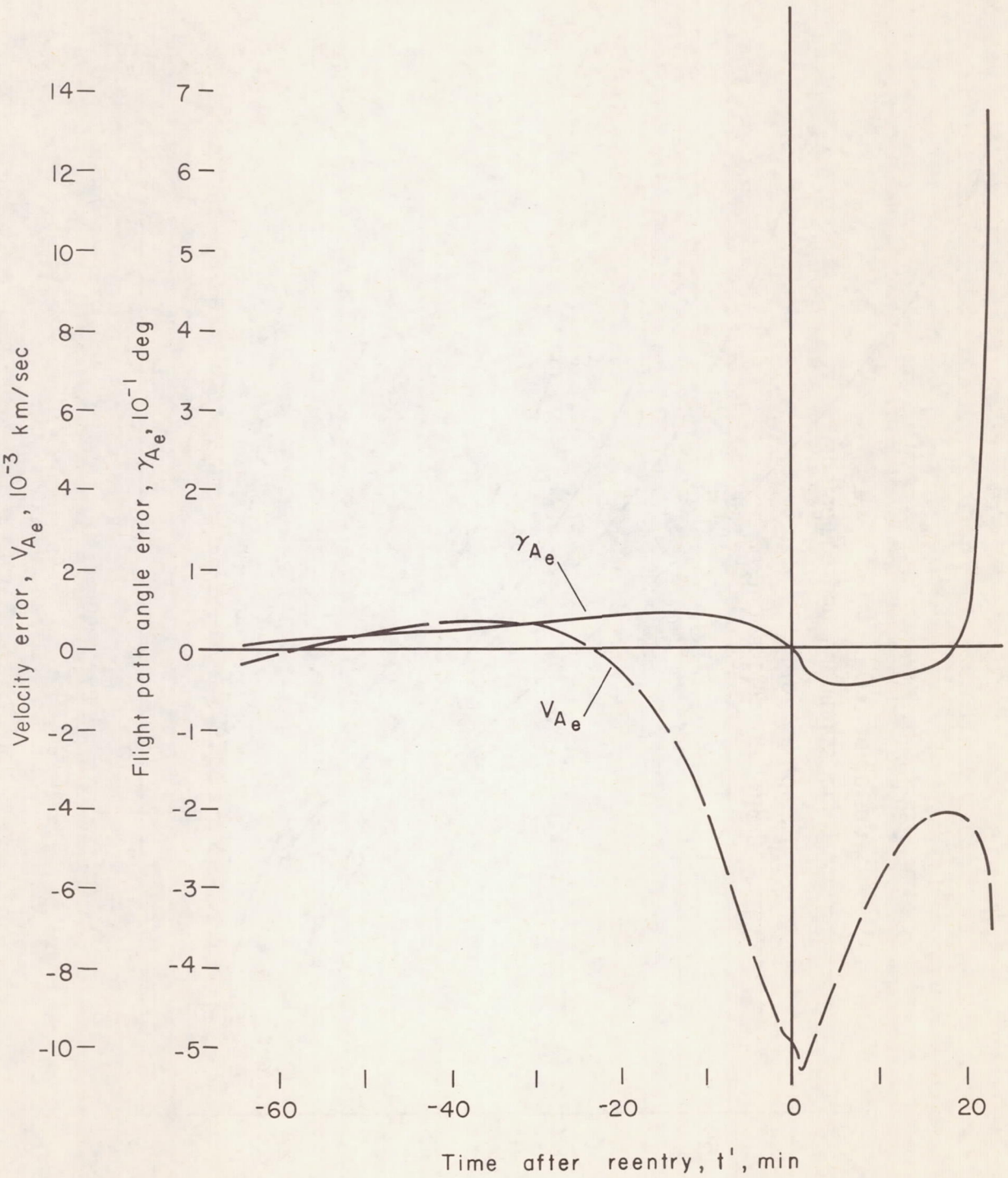

(b) Velocity and flight path angle errors.

Figure 3.- Concluded.

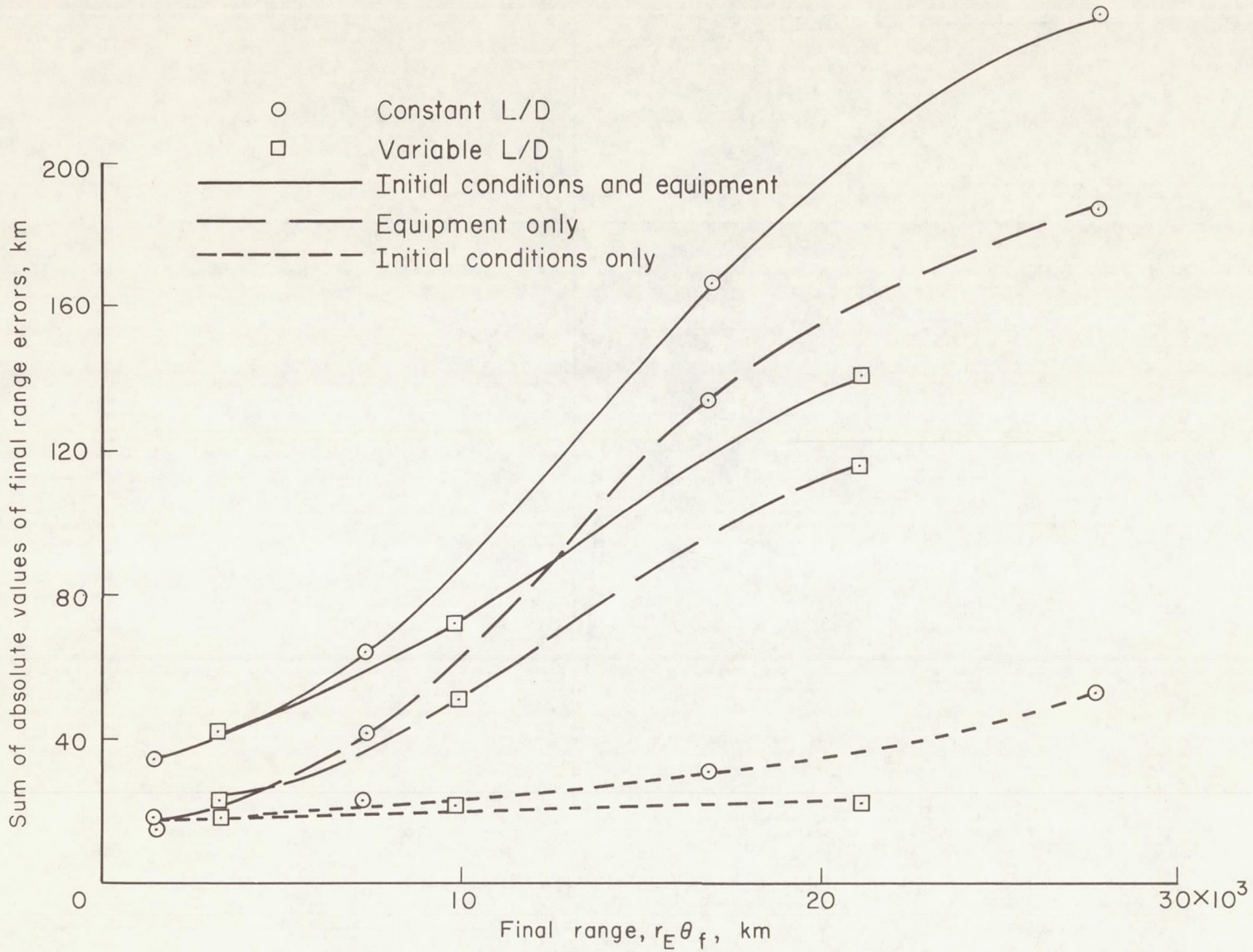

(a) Final range errors.

Figure 4.- Sum of the absolute values of final position errors versus final range.

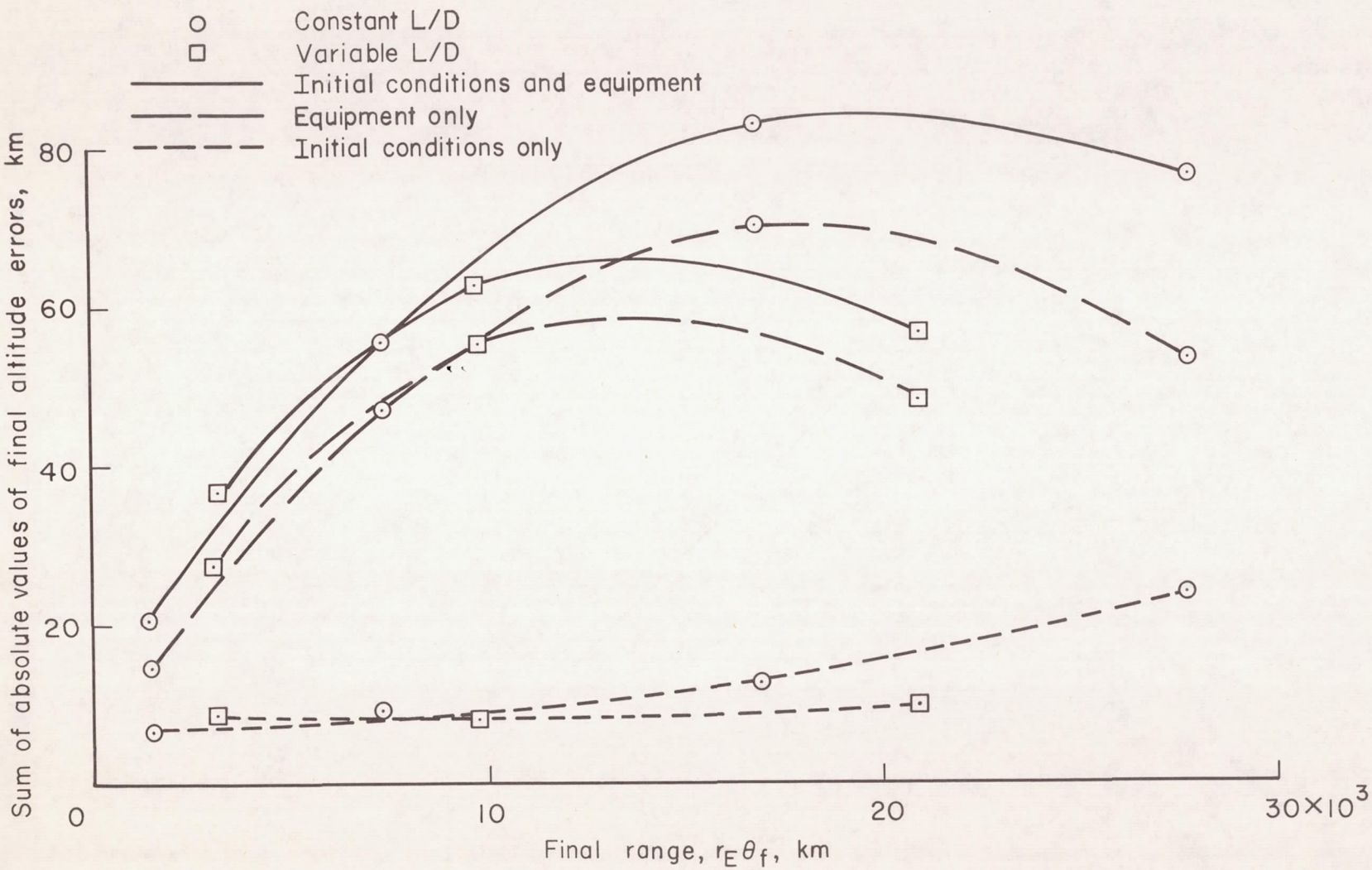

(b) Final altitude errors.

Figure 4.- Concluded.

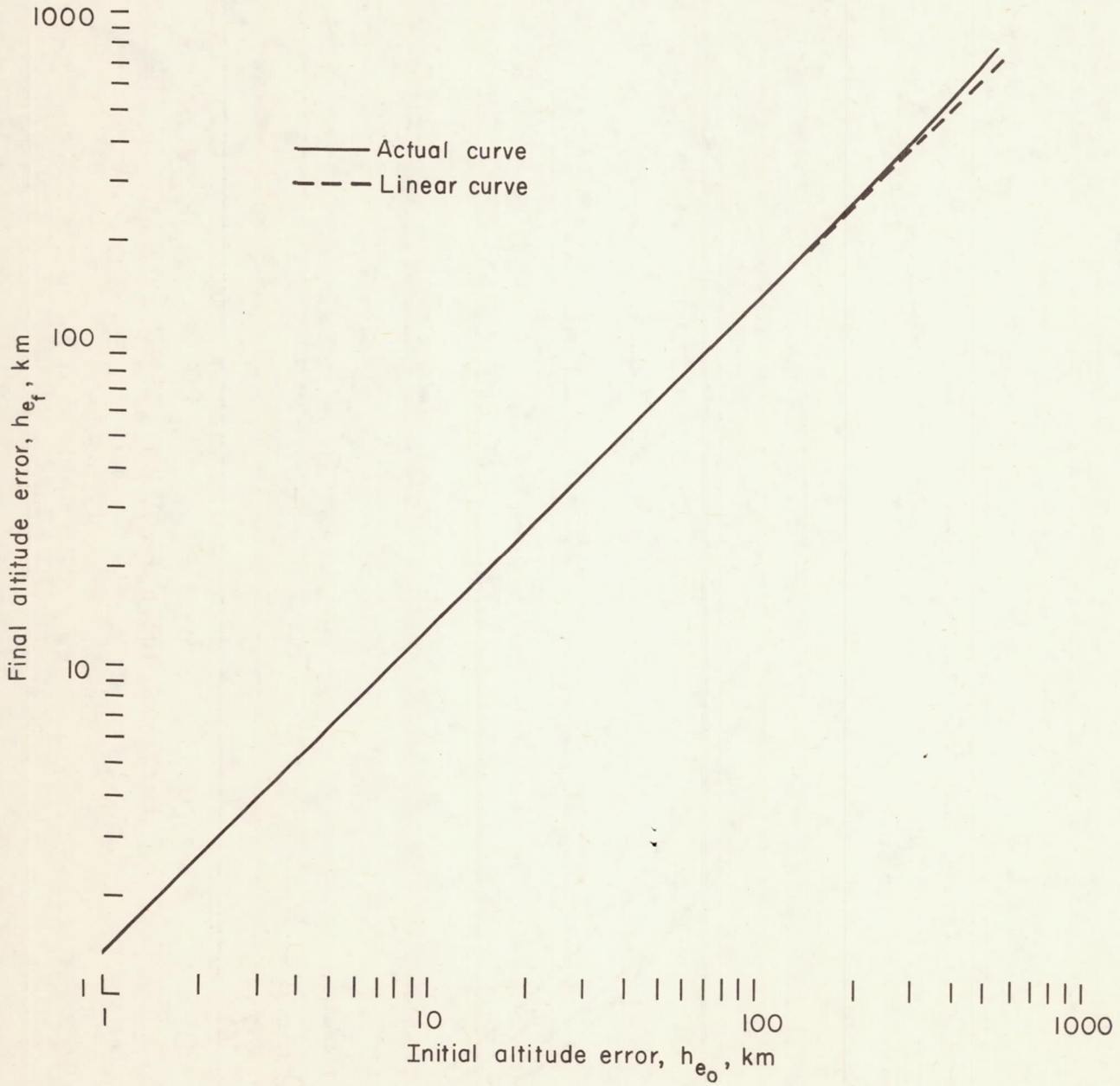

(a) Final altitude error versus initial altitude error.

Figure 5.- Error linearity.

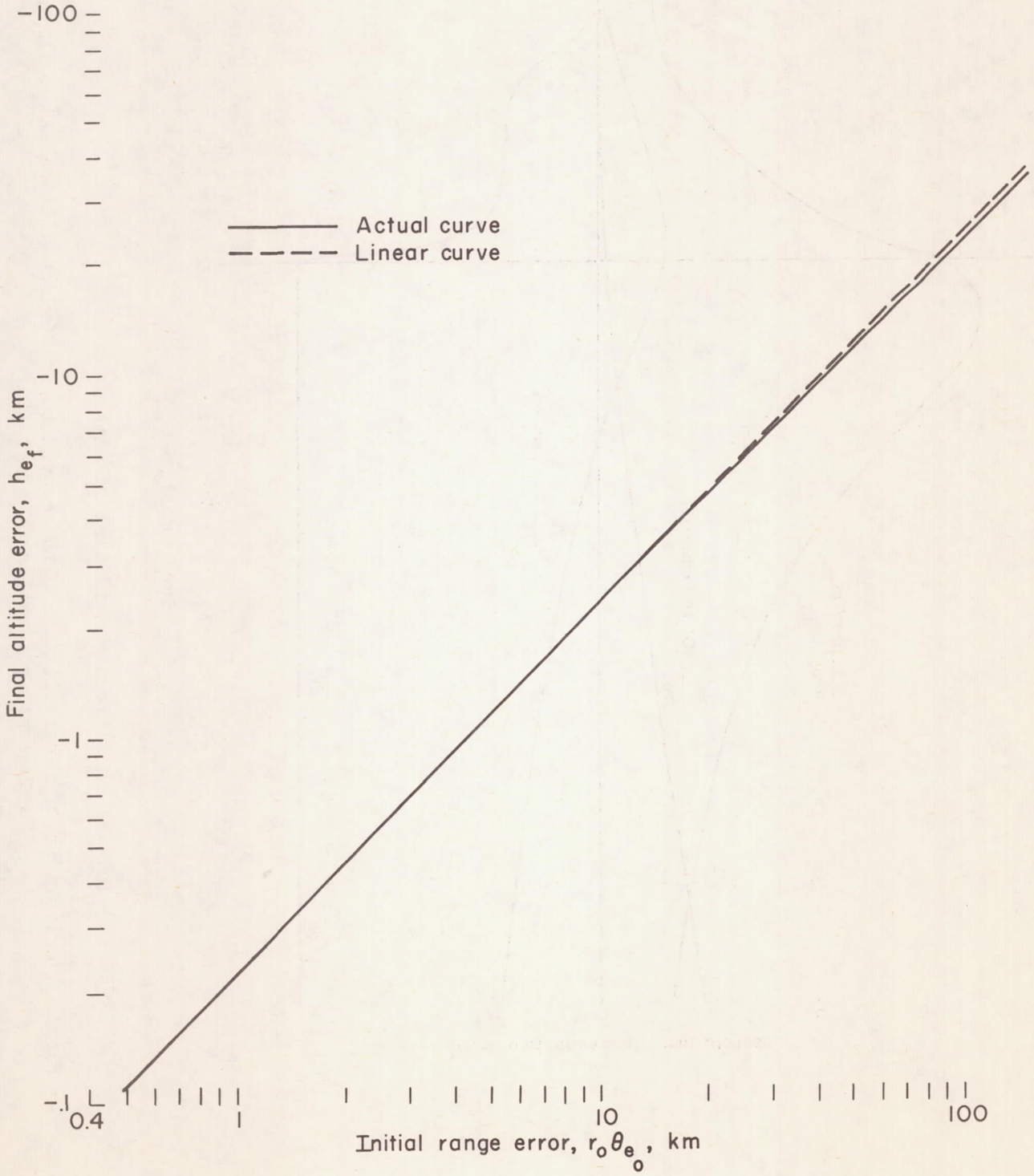

(b) Final altitude error versus initial range error.

Figure 5.- Concluded.

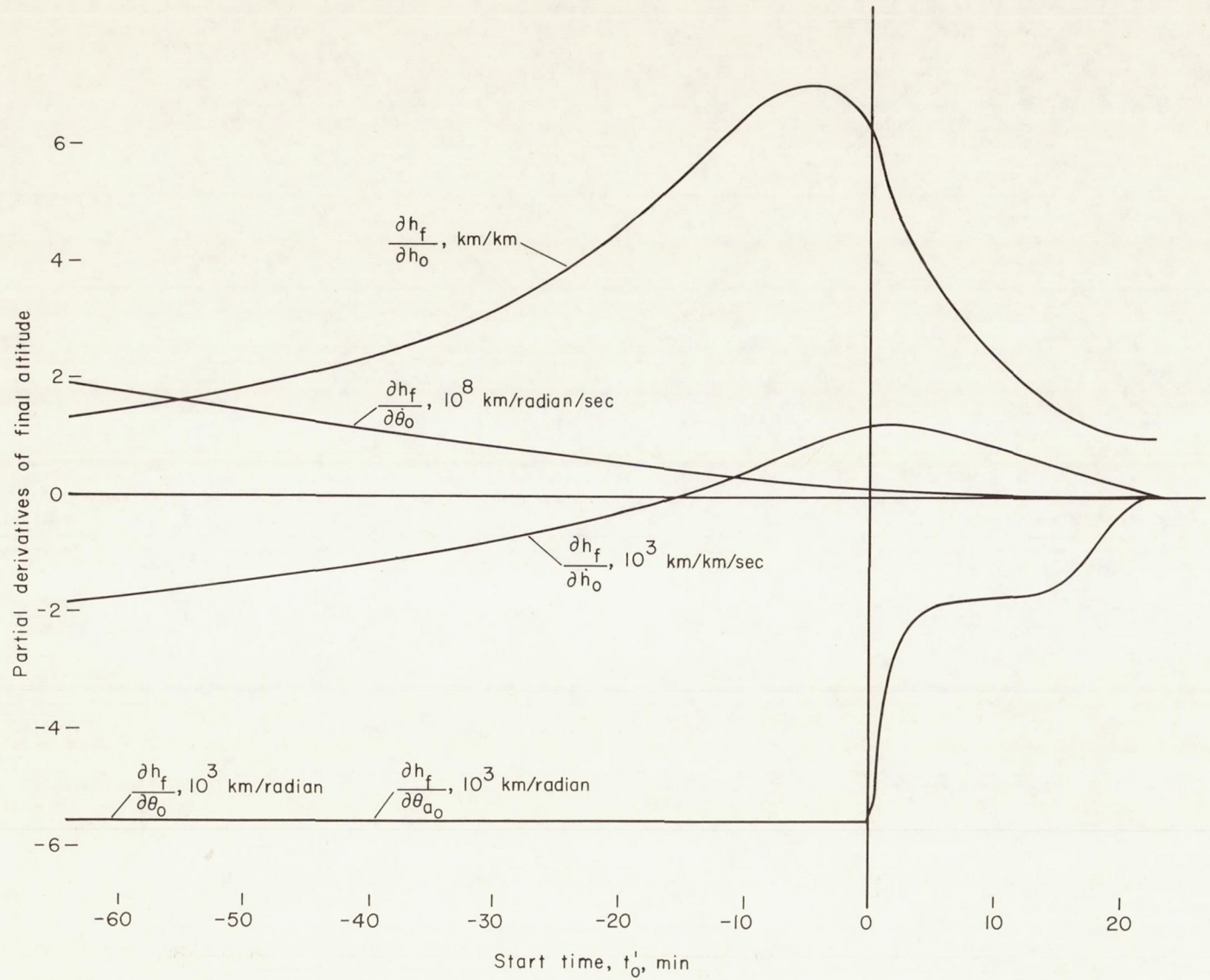

(a) Initial conditions and initial misalinement angle.

Figure 6.- Partial derivatives of final altitude with respect to initial conditions and equipment parameters as function of start time.

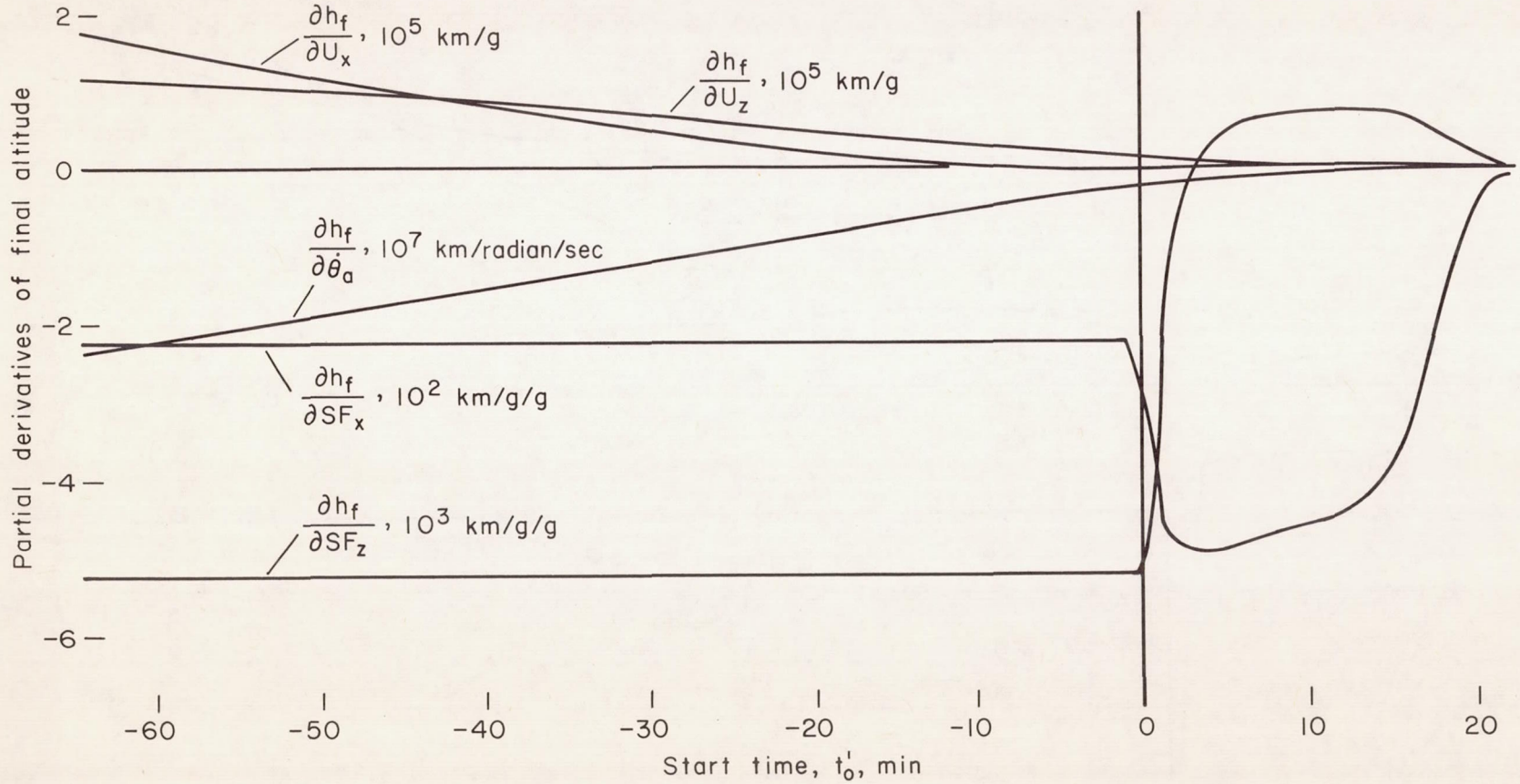

(b) Equipment parameters except for initial misalinement angle.

Figure 6.- Concluded.

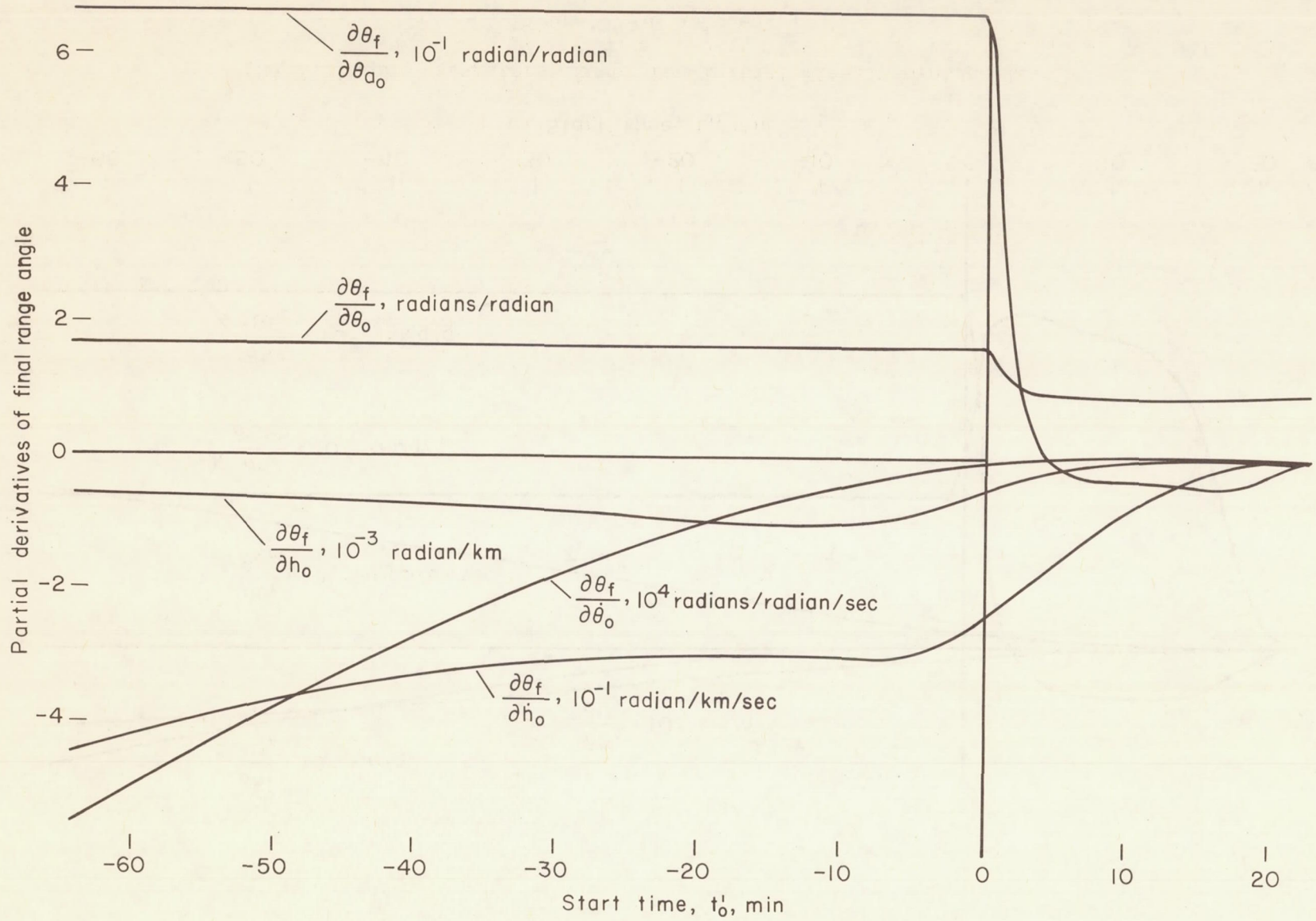

(a) Initial conditions and initial misalinement angle.

Figure 7.- Partial derivatives of final range angle with respect to initial conditions and equipment parameters as function of start time.

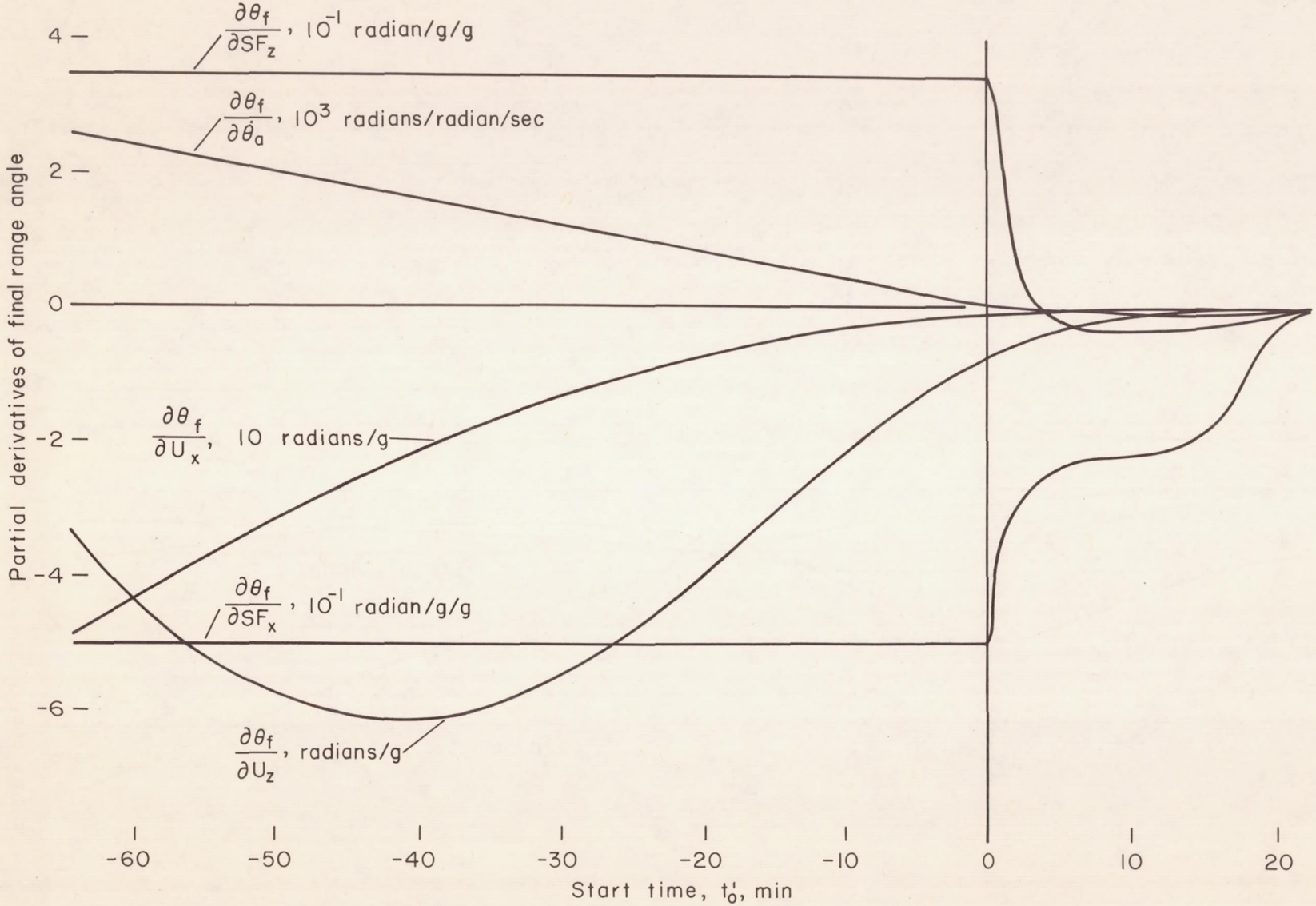

(b) Equipment parameters except for initial misalinement angle.

Figure 7.- Concluded.

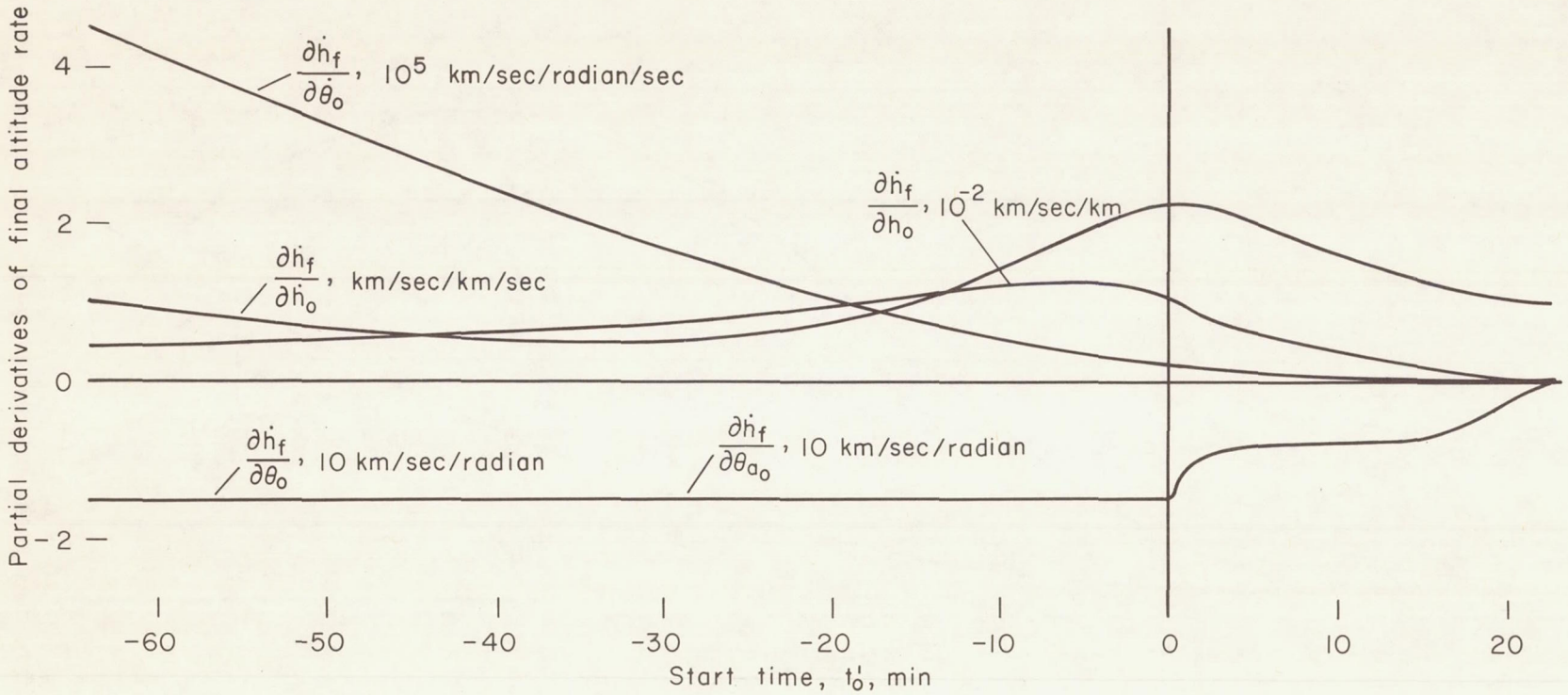

(a) Initial conditions and initial misalinement angle.

Figure 8.- Partial derivative of final altitude rate with respect to initial conditions and equipment parameters as function of start time.

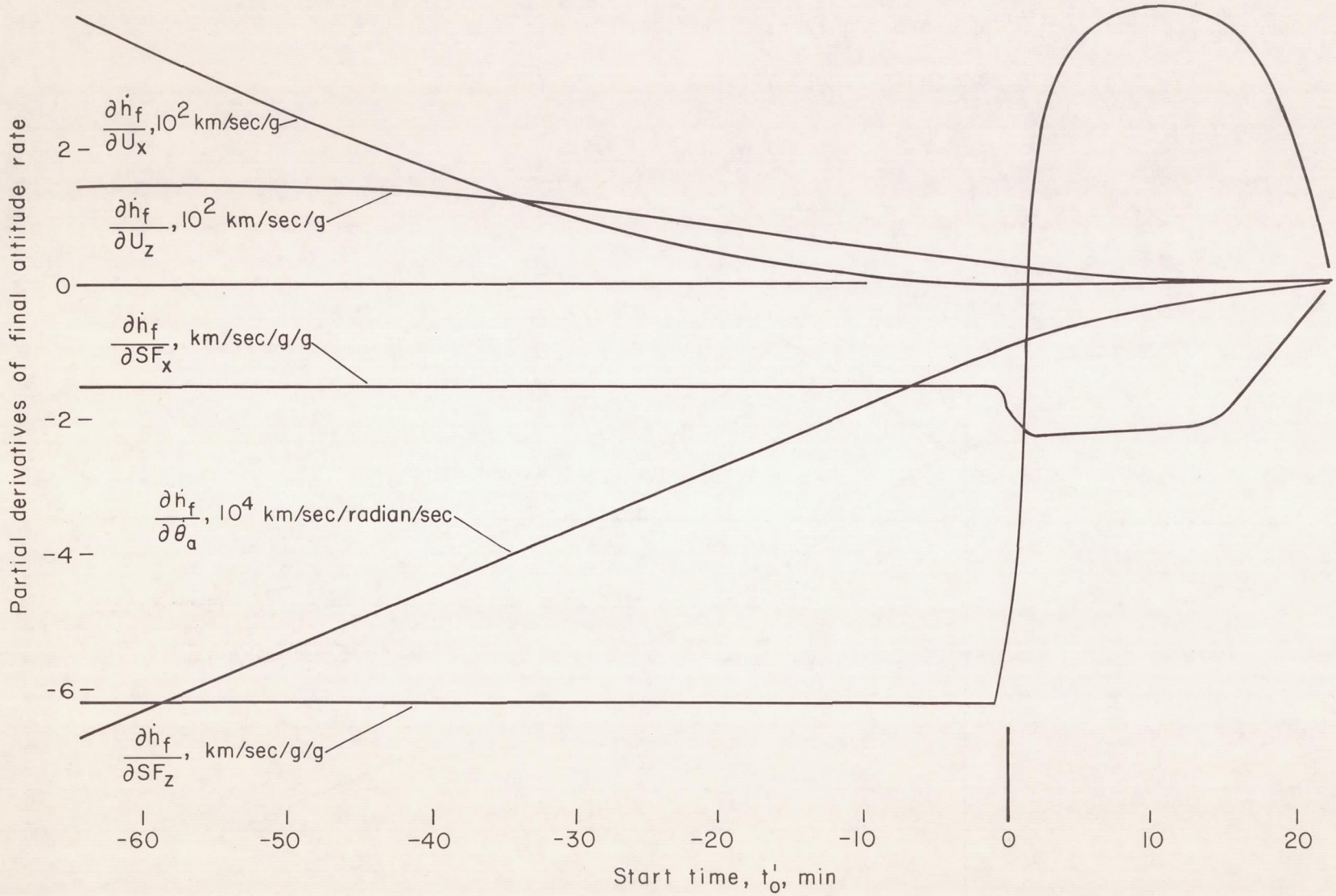

(b) Equipment parameters except for initial misalinement angle.

Figure 8.- Concluded.

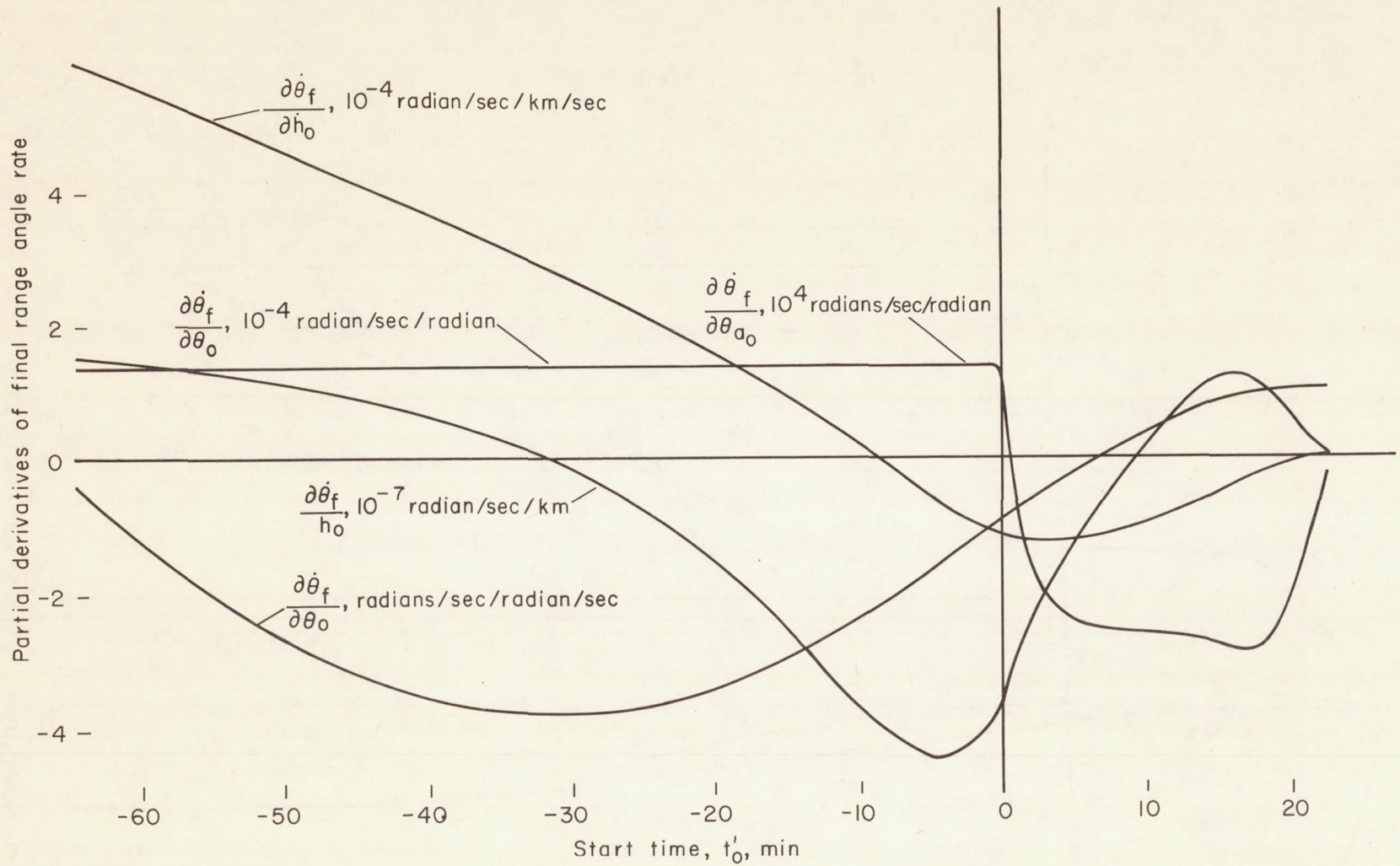

(a) Initial conditions and initial misalinement angle.

Figure 9.- Partial derivatives of final range-angle rate with respect to initial conditions and equipment parameters as function of start time.

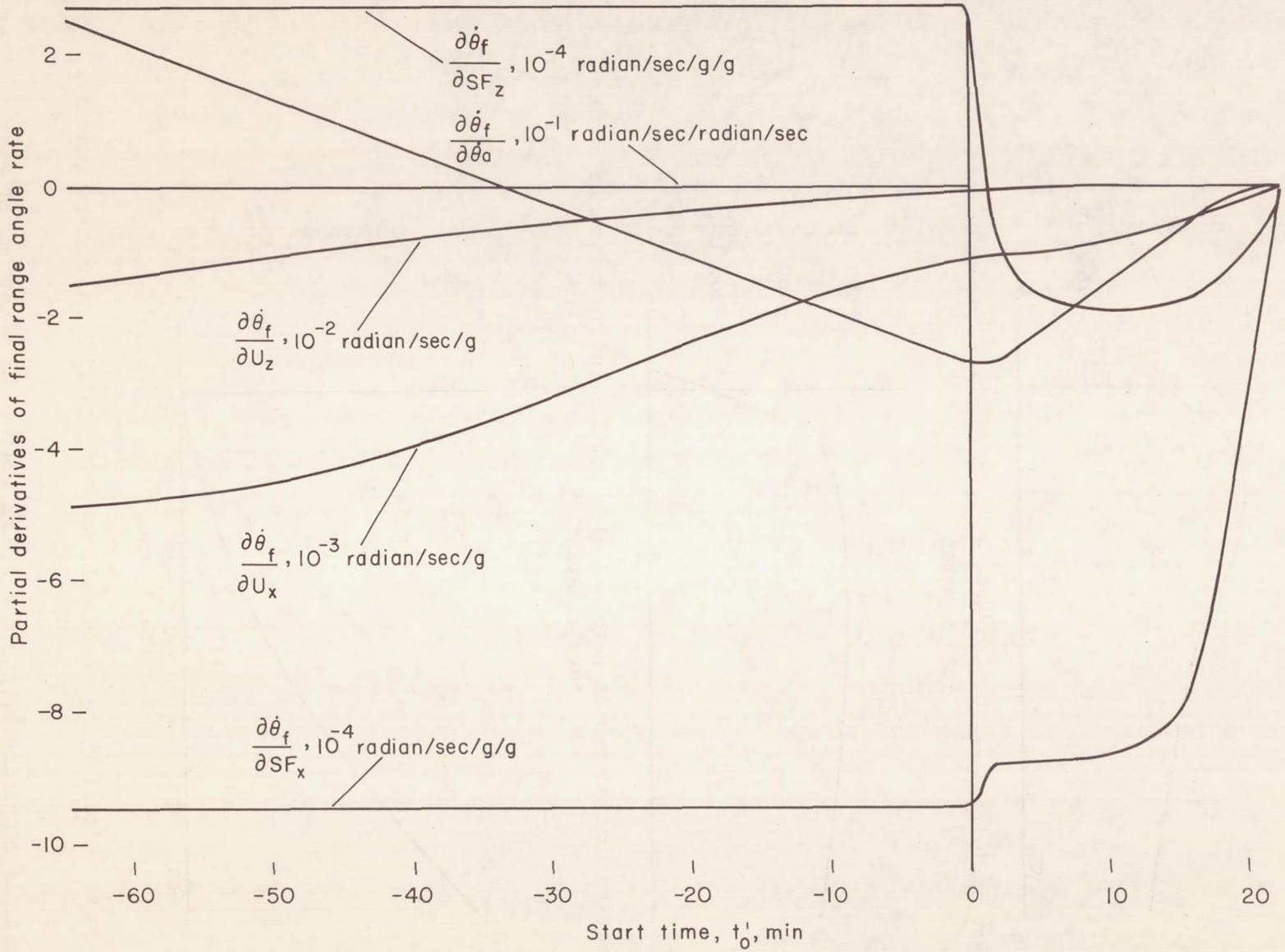

(b) Equipment parameters except for initial misalinement angle.

Figure 9.- Concluded.

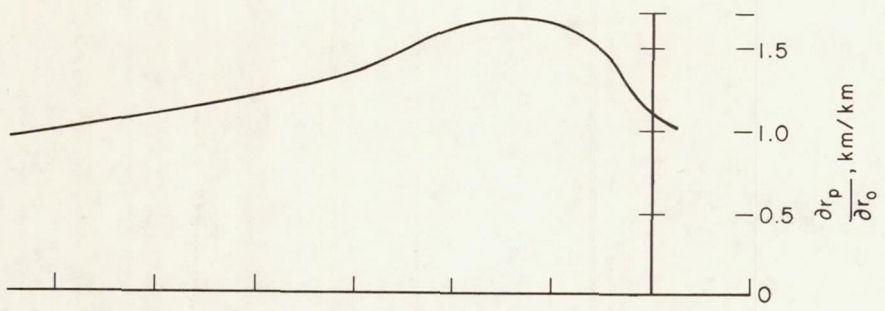

(a) With respect to initial radius and with initial radius rate and range angle rate constant.

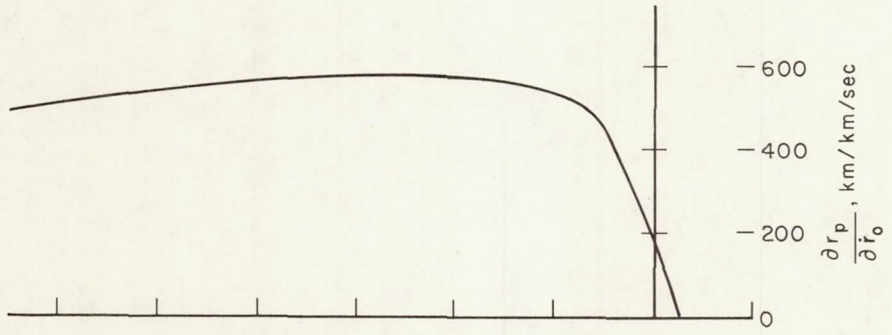

(b) With respect to initial radius rate and with initial radius and range angle rate constant.

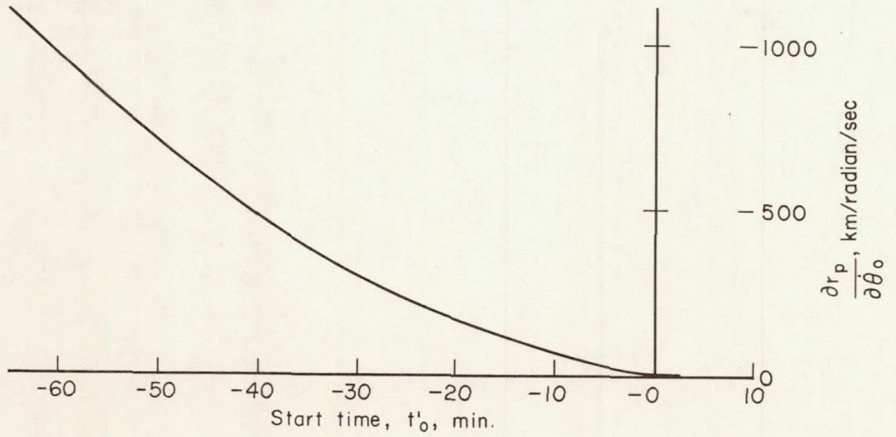

(c) With respect to initial range angle rate and with initial radius and radius rate constant.

Figure 10.- Partials of radius of perigee for an ellipse as functions of start time using radius, radius rate, and range angle rate as variables.

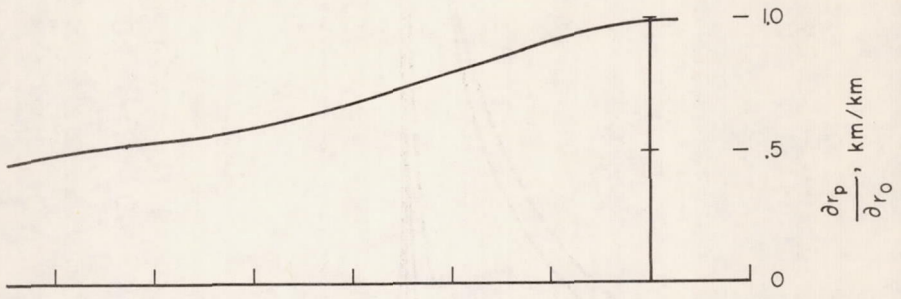

(a) With respect to initial radius and with initial velocity and flight-path angle constant.

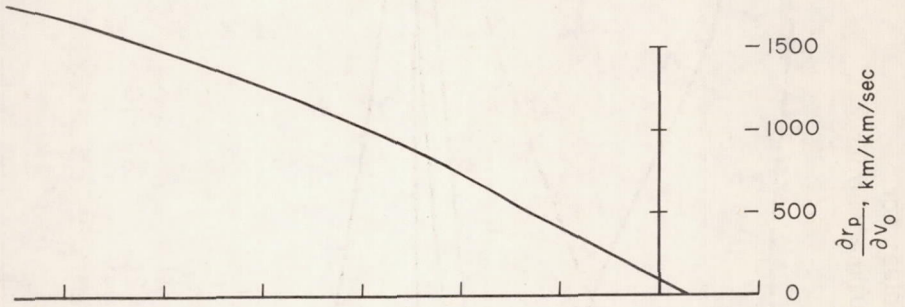

(b) With respect to initial velocity and with initial radius and flight-path angle constant.

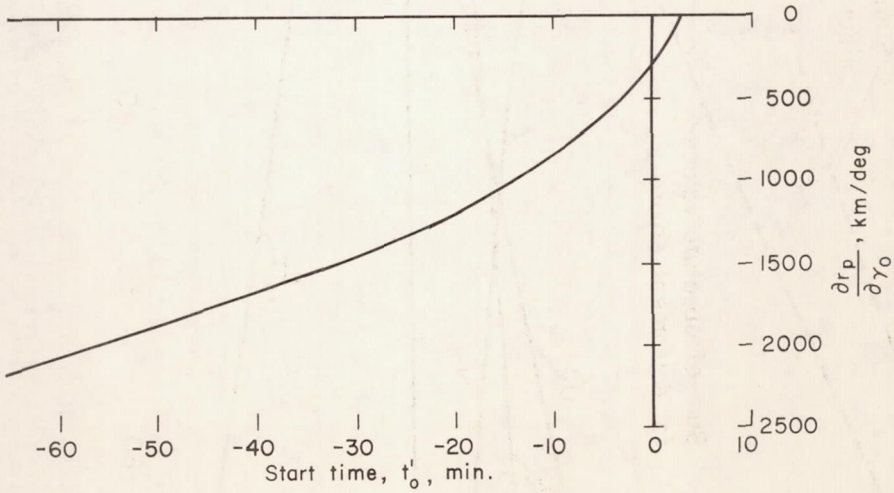

(c) With respect to initial flight-path angle and with initial radius and velocity constant.

Figure 11.- Partials of radius of perigee for an ellipse as functions of time using radius, velocity, and flight-path angle as variables.

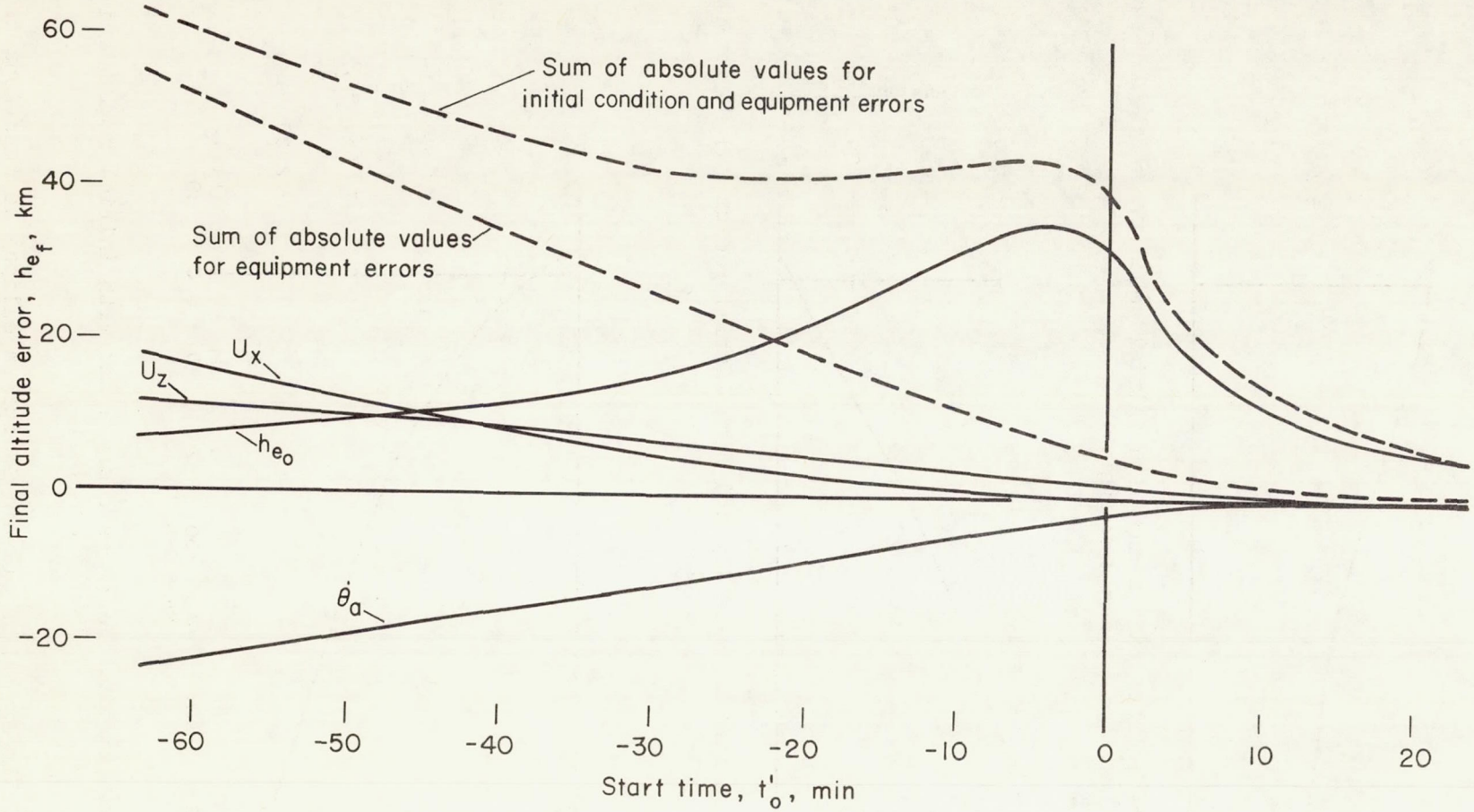

(a) Final altitude error.

Figure 12.- Final errors versus start time.

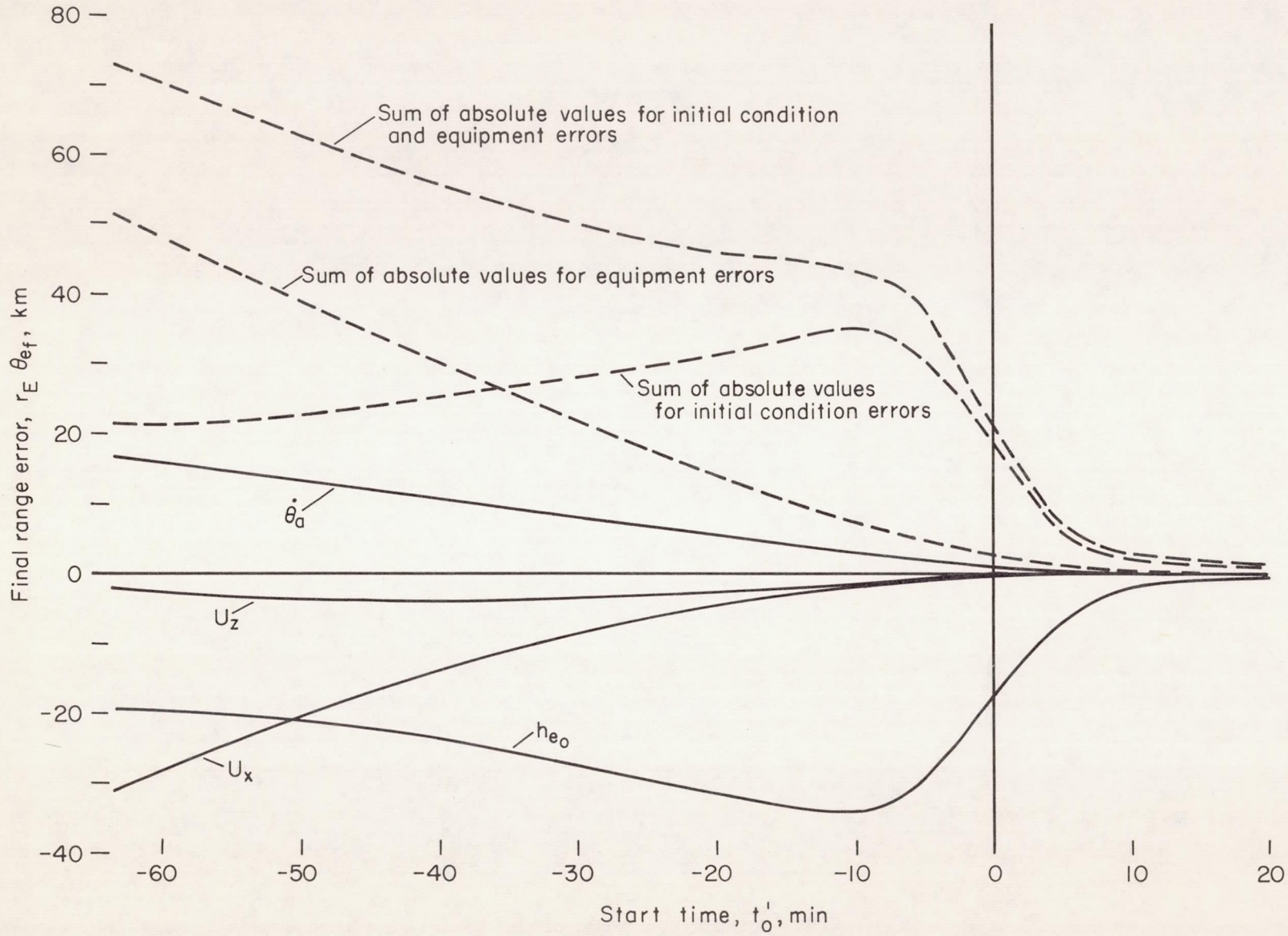

(b) Final range errors.

Figure 12.- Concluded.